AD-762 318

INFRARED EMISSION FROM ELECTRON IRRADIATED AIR LABORATORY EXPERIMENT FEASIBILITY STUDY

Morton Camac

Utah State University

Prepared for:

Air Force Cambridge Research Laboratory
Defense Advanced Research Projects Agency

November 1972

DISTRIBUTED BY:

NTIS

National Technical Information Service
U. S. DEPARTMENT OF COMMERCE
5285 Port Royal Road, Springfield Va. 22151

BEST
AVAILABLE COPY

AD 762318

INFRARED EMISSION FROM ELECTRON IRRADIATED AIR LABORATORY EXPERIMENT FEASIBILITY STUDY

by

Morton Camac*

Electro-Dynamics Laboratory
Utah State University
Logan, Utah 84321

Contract No. F19628-70-C-0289
Project No. 8692

D D C
RECEIVED
JUN 25 1973
B

Special Scientific Report

November 1972

*Aerodyne Research, Inc.
Northwest Industrial Park
Burlington, Massachusetts 01803

Contract Monitor: Dean F. Kimball
Optical Physics Laboratory

Approved for public release; distribution unlimited.

Sponsored by

Defense Advanced Research Projects Agency
ARPA Order No. 1366

Monitored by

AIR FORCE CAMBRIDGE RESEARCH LABORATORIES
AIR FORCE SYSTEMS COMMAND
UNITED STATES AIR FORCE
BEDFORD, MASSACHUSETTS 01730

Reproduced by
NATIONAL TECHNICAL
INFORMATION SERVICE
U S Department of Commerce
Springfield VA 22151

60

ARPA Order No. 1366

Program Code No. 2E50

Contractor: Utah State University

Effective Date of Contract: 1 June 1970

Contract No. F19628-70-C-0289

Principal Investigator and Phone No.
Dr. Doran J. Baker/801 852-4100

AFCRL Project Scientist and Phone No.
Dean F. Kimball/617 861-3671

Contract Expiration Date: 30 April 1974

ACCESSION for
NTIS White Section ☑
DDC Buff Section ☐
UNANNOUNCED ☐
JUSTIFICATION .....
BY .....
DISTRIBUTION/AVAILABILITY CODES
Dist. AVAIL. and/or SPECIAL
A

Qualified requestors may obtain additional copies from the Defense Documentation Center. All others should apply to the National Technical Information Service.

UNCLASSIFIED
Security Classification

DOCUMENT CONTROL DATA - R&D

(Security classification of title, body of abstract and indexing annotation must be entered when the overall report is classified)

1. ORIGINATING ACTIVITY *(Corporate author)*
Utah State University
Electro-Dynamics Laboratory
Logan, Utah 84321

2a. REPORT SECURITY CLASSIFICATION
Unclassified

2b. GROUP

3. REPORT TITLE
INFRARED EMISSION FROM ELECTRON IRRADIATED AIR LABORATORY EXPERIMENT FEASIBILITY STUDY

4. DESCRIPTIVE NOTES *(Type of report and inclusive dates)*
Scientific. Interim.

5. AUTHOR(S) *(First name, middle initial, last name)*
Morton Camac

6. REPORT DATE
November 1972

7a. TOTAL NO. OF PAGES
~~64~~ 60

7b. NO. OF REFS
11

8a. CONTRACT OR GRANT NO. ARPA Order No. 1366
F19628-70-C-0289

b. PROJECT, TASK, WORK UNIT NOS.
8692 n/a n/a

c. DOD ELEMENT 62301D

d. DOD SUBELEMENT n/a

9a. ORIGINATOR'S REPORT NUMBER(S)
Special Scientific Report No. 2

9b. OTHER REPORT NO(S) *(Any other numbers that may be assigned this report)*
AFCRL-TR-73-0198 ARI-RR1

10. DISTRIBUTION STATEMENT
A – Approved for public release; distribution unlimited.

11. SUPPLEMENTARY NOTES
This research was sponsored by the Defense Advanced Research Projects Agency.

12. SPONSORING MILITARY ACTIVITY
Air Force Cambridge Research Laboratory (OP)
L. G. Hanscom Field
Bedford, Massachusetts 01730

13. ABSTRACT

A laboratory measurements program to simulate many chemical and radiative processes present at auroral altitudes is evaluated. An electron beam would be used to irradiate O_2 - N_2 mixtures, either pure or with O_3, NO, CO_2 or H_2O additives and measurements then made of the resultant ultraviolet, visible, and infrared emissions from the gas. The spatial distribution of the electron beam energy deposition would be obtained from the $N_2(1-)$ emission. The concentrations of metastable species would be determined from their emission. A major objective would be the investigation of infrared emission from air irradiated by ionizing radiation. Reactions between N and O_2 produce NO, an important source of infrared. Three-body recombination produces vibrationally active O_3 and NO_2. With the addition of CO_2 and H_2O, their characteristic infrared emission either excited directly by the electron beam or by vibration transfer from N_2 or O_2 would be observed. Estimates of the infrared emission from these molecules are presented as a function of pressure and electron beam current. The degree of ionization of the gas is low due to rapid dissociative recombination.

The operating range of the experiment is investigated. The low pressure limit is determined by diffusion losses to the wall. The high pressure limit is set by three-body reactions at low beam power and by thermal convection losses at high power. To avoid thermal convection produced by excessive gas heating the electron beam current must be below 100 miliamperes.

DD FORM 1 NOV 65 1473

UNCLASSIFIED
Security Classification

14. KEY WORDS	LINK A ROLE	LINK A WT	LINK B ROLE	LINK B WT	LINK C ROLE	LINK C WT
Infrared Emission						
Electron Excitation						
Electron Induced Emission						
Electron Beam						
Auroral Emission						

INFRARED EMISSION FROM ELECTRON IRRADIATED AIR
LABORATORY EXPERIMENT FEASIBILITY STUDY

by

Morton Camac*

Electro-Dynamics Laboratory
Utah State University
Logan, Utah 84321

Contract No. F19628-70-C-0289
Project No. 8692

Special Scientific Report

November 1972

*Aerodyne Research, Inc.
Northwest Industrial Park
Burlington, Massachusetts 01803

Contract Monitor: Dean F. Kimball
Optical Physics Laboratory

Approved for public release; distribution unlimited.

Sponsored by

Defense Advanced Research Projects Agency
ARPA Order No. 1366

Monitored by

AIR FORCE CAMBRIDGE RESEARCH LABORATORIES
AIR FORCE SYSTEMS COMMAND
UNITED STATES AIR FORCE
BEDFORD, MASSACHUSETTS 01730

ie

ABSTRACT

A laboratory measurements program to simulate many chemical and radiative processes present at auroral altitudes is evaluated. An electron beam would be used to irradiate O_2 - N_2 mixtures, either pure or with O_3, NO, CO_2 or H_2O additives and measurements then made of the resultant ultraviolet, visible, and infrared emissions from the gas. The spatial distribution of the electron beam energy deposition would be obtained from the $N_2[1-]$ emission. The concentrations of metastable species would be determined from their emission. A major objective would be the investigation of infrared emission from air irradiated by ionizing radiation. Reactions between N and O_2 produce NO, an important source of infrared. Three-body recombination produces vibrationally active O_3 and NO_2. With the addition of CO_2 and H_2O, their characteristic infrared emission either excited directly by the electron beam or by vibration transfer from N_2 or O_2 would be observed. Estimates of the infrared emission from these molecules are presented as a function of pressure and electron beam current. The degree of ionization of the gas is low due to rapid dissociative recombination.

The operating range of the experiment is investigated. The low pressure limit is determined by diffusion losses to the wall. The high pressure limit is set by three-body reactions at low beam power and by thermal convection losses at high power. To avoid thermal convection produced by excessive gas heating the electron beam current must be below 100 milliamperes.

Preceding page blank

TABLE OF CONTENTS

Section		Page
	ABSTRACT	iii
1	INTRODUCTION	1
2	THEORY OF EXPERIMENT	3
	2.1 Electron Beam Operation	9
	2.2 Measurement of Gas Temperature, Density, and Species	20
	2.3 Circulation Effects in the Tank	20
3	EXPERIMENTAL APPARATUS	23
	3.1 Chemistry Produced by the Electron Beam	26
4	INFRARED EMISSION FROM THE GAS	35
	SUMMARY	51
	REFERENCES	53

Preceding page blank

LIST OF ILLUSTRATIONS

Figure		Page
1	The atmospheric pressure, temperature and mean-free-path as a function of altitude from 60 to 140 kms.	4
2	Major species concentrations in the atmosphere from 80 to 160 kms.	5
3	Low pressure limit for laboratory experiment. The molecular collision time t_c and time for particles to diffuse to the wall from the center t_w versus air pressure in microns. Tank radius is 50 to 150 cm.	8
4	(A) Measurements[2] of electron beam energy required for 34 inch range versus pressure. (B) Power law fits to the data of Hartman[2] and Cohn and Caldeonia.[6] The solid curves show the range of the experimental data. Dashed portions are extrapolations from the data.	10
5	Electron beam voltage as a function of pressure for 1, 2, 4 and 10 meters range, based on the data of Cohn & Caledonia.[6]	12
6	The cross section for ionization of nitrogen and oxygen by electrons. The cross section for excitation of the N_2^+ [B] (1st negative) and N_2 [C] (2nd positive) states.	13
7	The electron excited luminescent spectrum of air at 70 microns pressure. Electron energy is 850 eV. Data of Hartman.[2]	15
8	Vibrational energy diagram for CO_2, N_2, CO, H_2O, and O_2. The solid vertical lines are permitted radiative transitions. The arrows between states are the times for deactivation or vibration transfer for air at 100 microns pressure and at room temperature.	18
9	The rotation spectrum of the $N_2^+(1-)$ ($v' = 0$, $v'' = 0$) transition around the line center of 3914A.[10] An analysis which determines those rotational temperatures, equal to the translational temperature is also shown in this experiment.	21
10	The ratio of the intensities of vibration bands transitions of the N_2^+ [1-] system versus the N_2 vibrational temperature.[8] The sensitivity becomes linear above about 900 ^{o}K.	22

Preceding page blank

List of Illustrations (Cont.)

Figure		Page
11	Schematic of experimental arrangement for measuring the ultraviolet, visible and infrared emission from gas excited by an electron beam.	24
12	Several arrangements of the infrared optical system. (A) is for good focusing at the center of the tank; (B) is for focusing at the opposite wall so that a flow system can be used with a cool surface; (C) give details of the flow.	25
13	Thermal convective patterns with electron beam heating. The beam is confined to a core along the axis of the tank and is directed vertically or horizontally.	29
14	The time for thermal conduction and convection losses to the wall as a function of the gas pressure in torr. The tank radius is 0.5 and 1.5 meters. The beam current is 1, 10 and 100 milliamperes. The solid portion of the convection curve apply to both tank sizes, while the dashed portion applies to the 1.5 meter radius. The curves end where the analysis presented does not apply.	33
15	The time t_w for vibrationally excited nitrogen to diffuse to the wall as a function of the pressure. The time for N_2 vibrational energy to transfer to CO_2, for 3.4×10^{-4} and 10^{-2} CO_2 molefractions. When the wall is catalytic, the shorter time is appropriate for the experiment. Above 30 microns pressure the CO_2 radiating state is in equilibrium with the ground state, while at the lower pressures the population is depressed by radiation cooling.	39
16	The CO_2 4.3 micron emission as a function of air pressure for a 1 meter diameter tank and an electron beam current of 10 milliamperes. The two cases presented ar for a catalytic and non-catalytic wall to N_2 vibrational energy. For the non-catalytic wall, the excited nitrogen population builds up until transfer to CO_2. With the catalytic wall the transfer to CO_2 must occur before N_2 collisions with the wall. At low pressure the wall losses dominate, depressing the radiation.	41
17	The NO 5.3μ emission as a function of air pressure for a 1 meter diameter tank and 10 mamps electron beam current. The emission is due to the reaction $N(^2D) + O_2 \rightarrow NO(v) + O$ followed by 2.7 photons per reaction.	44
18	The O_3 9.6μ emission as a function of air pressure for a 1 meter tank and a 10 mamps electron beam current. The air contains 1% ozone. Three reactions were considered: vibration transfer from N_2 to O_3, direct O_3 vibration excitation by electrons, and the three-body recombination $O + O_2 + M \rightarrow O_3(v) + M$. The emission following the latter is below 10^{-13} watts/cm^2 sr.	45

Section 1

INTRODUCTION

There is a growing interest in determining atmospheric infrared emission in the 2 to 30 micron region under both quiescent and radiation disturbed conditions. Disturbed atmospheres occur naturally in the auroras, where the upper atmosphere is irradiated by electrons and protons. Infrared measurements by Murcray[1] indicate that infrared emission from aurora are enhanced by a factor of 50 over the quiescent atmospheric level.

High altitude balloons and rocket-borne field measurements of the auroral infrared radiation are either or presently underway. Laboratory experiments have been proposed to simulate some auroral situations, and guide the field measurements. This paper describes a laboratory experiment in which many of the chemical phenomena found in the upper atmosphere can be simulated.

The suggested experimental system would use a tank containing air at several microns pressure or above. The air would be irradiated with an electron beam of several hundred electron volts energy. The measurements would allow radical and metastable species to be monitored. The main source of information would be detailed electron-beam-excited spectral observations in the ultraviolet, visible and infrared.[2] The visible data would yield information about the air rotational and vibrational temperatures, as well as the concentrations of the major species. Additional types of measurements (not treated in this report) such as laser scattering from specific states and mass spectrometric identification of the ionic concentrations could also be made.

This experiment should yield three types of information: (1) calibration of electron luminescent spectra, (2) infrared emission from air at low pressure irradiated by electrons, and (3) air chemistry following electron excitation and dissociation. A variety of reactions could be investigated by adding other species, such as, O, NO and triatomic molecules to the air.

Section 2 describes the theory of the experiment. Section 3 presents details of the experimental arrangement. The concluding section estimates the infrared and visible signal intensities.

Section 2

THEORY OF EXPERIMENT

In the suggested experiment, low pressure air in a large tank would be irradiated with an electron beam. The primary measurements made would be of the air optical emission in the ultraviolet, visible and infrared. In determining an optimal experimental configuration several factors must be evaluated and this section considers the following areas: (1) air pressure range, (2) electron beam range, energy, and interaction with the air, (3) chemistry following electronic excitation, (4) effect of diffusion of ions, radicals and excited species to the wall, and (5) convection currents in the gas due to temperature gradients.

Before describing the experimental conditions, some of the properties of the upper atmosphere will be reviewed. Figure 1 presents the atmospheric pressure, temperature, and mean-free-path for momentum transfer from 60 to 140 km. Note that the temperature remains around 200°K until 100 km and then quickly rises, becoming 620°K at 140 km. The mean-free-path varies from 0.28 mm at 60 km to 16 meters at 140 km.

Figure 2 shows the concentrations of the major atmospheric species over the range from 60 to 160 km.[3] The noble gases such as argon and helium are not considered since they do not affect the infrared emission. In addition to the ground states, the metastable state of many species are populated at low levels. These play an important role in upper atmospheric chemistry. A number of metastable electronic states and their radiative lifetimes[4] are listed in Table 1. Also presented are the pressures and corresponding altitudes at which the collisional deactivation time τ_{col} equals the radiative lifetime.

The upper atmospheric chemistry including metastable species and minor constituents is extensive and many reaction rates are uncertain. The review by Bortner and Kummler[5] illustrates the problems involved in defining the total number of reactions and the complete atmospheric chemistry. In this paper, we consider some of the major processes leading to infrared emission. Because of the reaction rate uncertainties, some important processes could be missing.

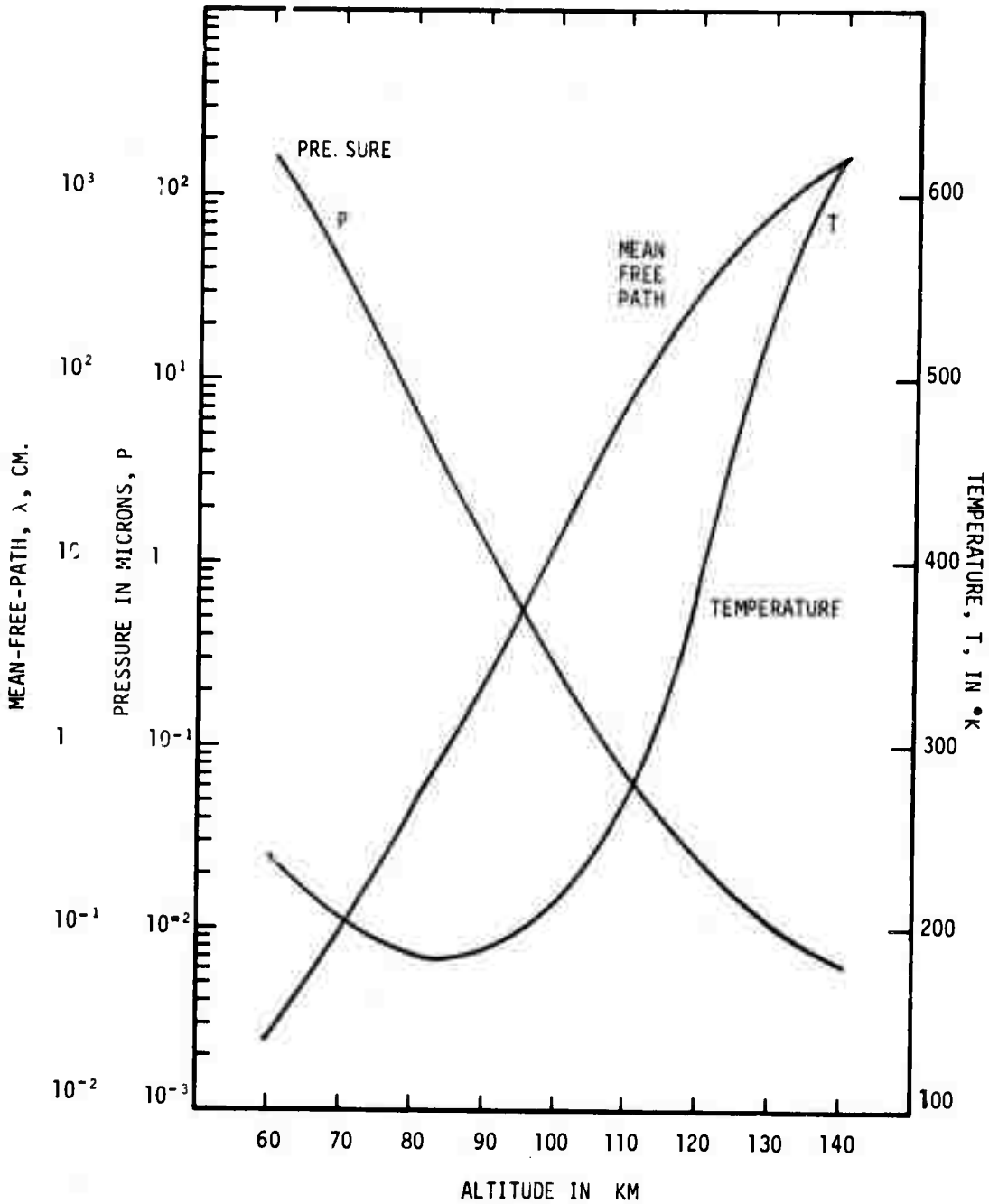

Figure 1. The atmospheric pressure, temperature and mean-free-path as a function of altitude from 60 to 140 kms.

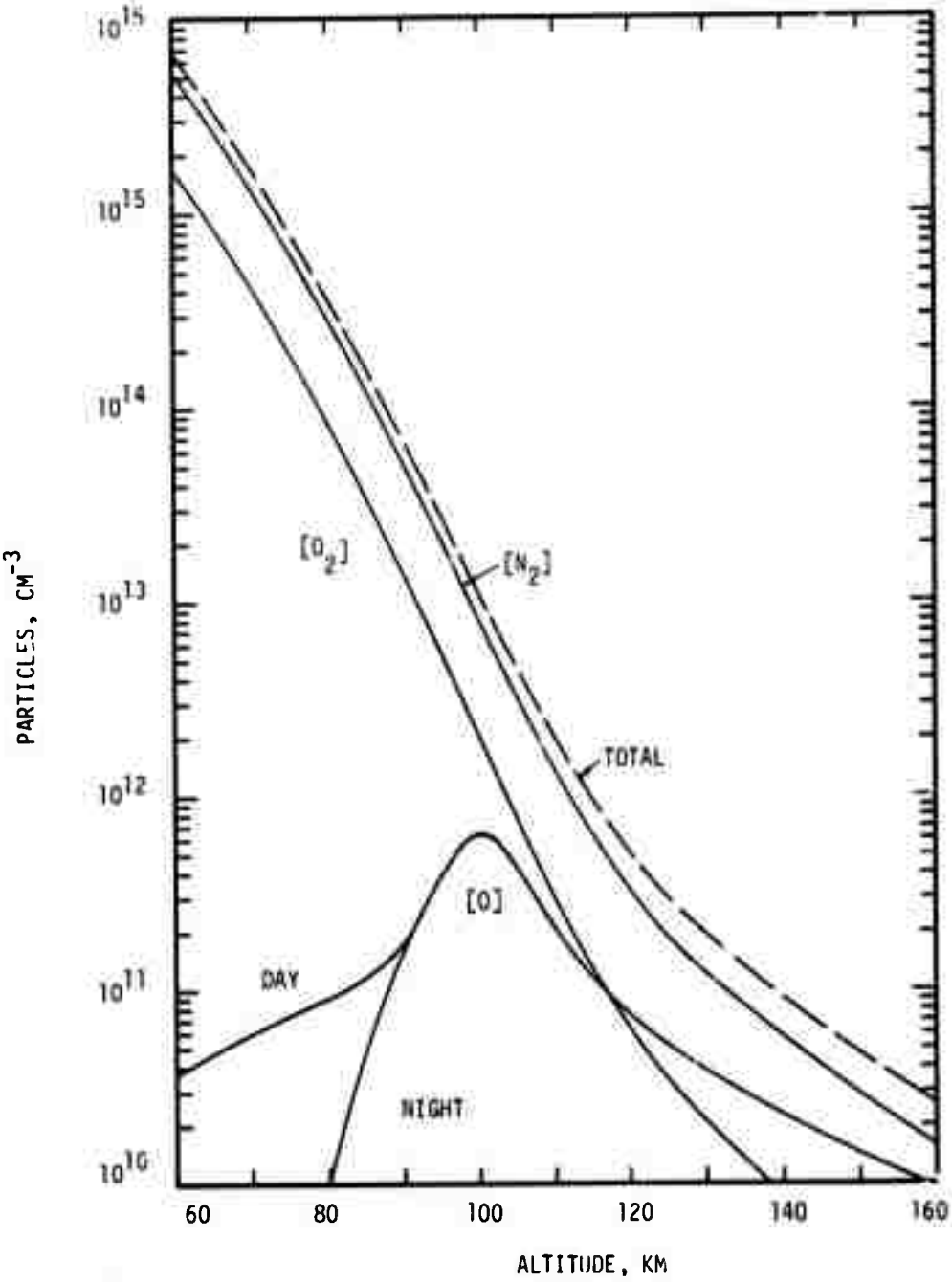

Figure 2. Major species concentrations in the atmosphere from 80 to 160 kms.

TABLE 1. RADIATIVE LIFETIMES[4]

Metastable Species	Radiative Lifetime	Pressure, microns $\tau_{col} = \tau_{rad}$	Altitude, km $\tau_{col} = \tau_{rad}$
O_2 ($a^1\Delta g$)	45 min	580	60
O_2 ($b^2\Sigma' g^+$)	12 sec	1.63	91
N_2 ($A^3\Sigma_u^+$)	2 sec	.81	96
N (^2D)	26 hrs	1.7×10^{-6}	360
N (^2P)	12 sec	-	-
O (^1S)	.75 sec	1.03	95
O (^1D)	110 sec	2.82×10^{-3}	130
O^+ (^2P)	5 sec		
O^+ (^2D)	3.6 hrs		
N^+ (^1S)	0.90 sec		
N^+ (^1D)	4.13 min		

The atmospheric parameters should be compared with the operating range of laboratory experiments. Since the collision mean-free-path must be much smaller than the tank dimensions, this sets the minimum operating pressure in a laboratry experiment. It will be shown that the minimum operating pressure is above several microns, corresponding to the pressure around 90 km altitude.

The lower operating pressure in a laboratory experiment is set by the ratio of the collision mean-free-path to the size of the apparatus. The excited particles and radicals should be kept in the vicinity of the optical system for times comparable to the reaction times leading to infrared emission. At low pressures, the reaction times could be seconds, and the excited air species should not undergo wall collisions for comparable lengths of time.

Consider a cylindrical tank containing air at a pressure p. A particle would tranverse the tank in a time t_w given approximately by the relation

$$t_w \approx R^2/\lambda c \tag{1}$$

where R is the radius of the tank, λ is the collision mean-free-path and c is the thermal velocity of the particles. For nitrogen at room temperature the thermal velocity is 3.4×10^4 cm/sec, and the mean-free-path, λ, is (5/p) cm where p is the pressure in microns of Hg. Figure 3 shows t_w, as a function of pressure for two tank sizes: 50 cm and 150 cm. Also shown in Figure 3 is the time between collisions, t_c,

$$t_c = \lambda/c = 5/3.4 \times 10^4 p = (150/p) \text{ microseconds} \tag{2}$$

The ratio of times is simply

$$t_w/t_c \approx (R/\lambda)^2 = (0.2Rp)^2 \tag{3}$$

The two tank sizes permit operation down to pressures between 1 and 10 microns. For example, with the 50 cm tank at 10 microns pressure, the collision time t_c is 150/10 = 15 μsec, while the diffusion time to the wall t_w is $(0.2 \times 50 \times 10)^2 = 10^4$ times longer, or 0.15 seconds, for the 150 cm tank at 1 micron pressure, t_c = 150 μsec and t_w = 0.14 sec. Reactions that require up to a second could be studied at these pressures while reactions of a longer duration should be studied at higher pressures.

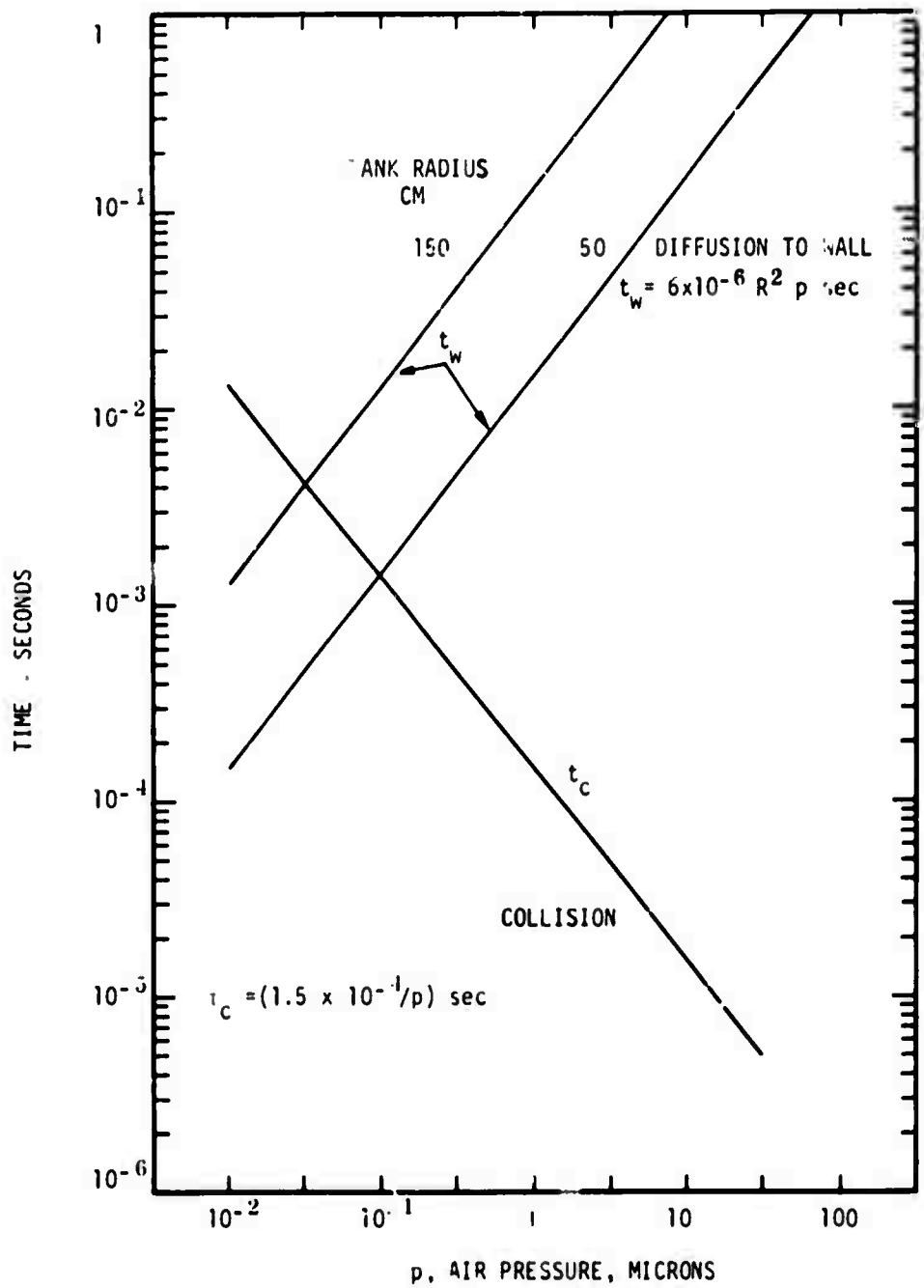

Figure 3. Low pressure limit for laboratory experiment. The molecular collision time t_c and time for particles to diffuse to the wall from the center t_w versus air pressure in microns. Tank radius is 50 to 150 cm.

Two difficulties which could arise in extrapolating the high pressure ($\geq$ 10 micron) data in the laboratory experiment to the low ($\leq$ 0.3 micron) pressures in the upper atmosphere are: (1) collisional quenching of chemically important metastable states, and (2) three body collision reaction which form triatomic molecules or negative ions. Three body reactions forming neutral triatomic species are extremely slow at 100 microns pressure and would not complicate the experiment. On the other hand, negative ion formation progresses rapidly and can determine the upper operating pressure. At low beam currents the upper pressure range is about 10μ, while above 10 milliampere per square centimeter the operating pressure is in excess of 100μ

At very low pressures radiative transitions deplete metastables before collisions. However, at higher pressure, collisional deactivation of metastables becomes important causing more chemistry involving metastable species. This experimental difficulty could be calibrated out after the process is identified, since the deactivation and radiative rates for the metastable states are known.

2.1 Electron Beam Operation

The range of low energy electrons in air has been studied by Hartman[2] and Cohn and Caledonia.[6] At each electron beam energy, Hartman[2] measured the pressure at which the range is 34 inches; see Figure 4A. A simple power law fit to these data gives

$$R_e = \begin{cases} 0.48\ E^{4/3}/p \ \text{cm} & \text{for } 125 < E < 1000 \\ 0.027\ E^{7/4}/p \ \text{cm} & \text{for } 1000 < E < 1350 \end{cases} \tag{4}$$

where R_e is the range of the electron beam in cm; E is the electron energy in electron volts; and p is the pressure in microns. This formula fits the data in Figure 4 from about 125 eV to 1350 eV. Below 125 eV, the data indicate a larger range than that obtained from Equation (4). Cohn and Caledonia[6]

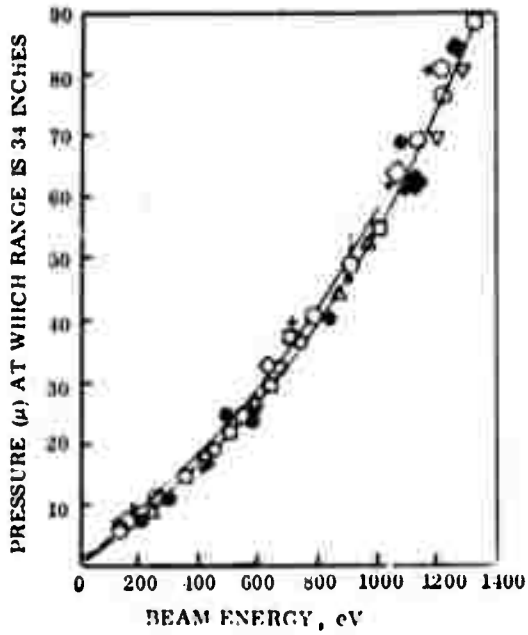

(A)

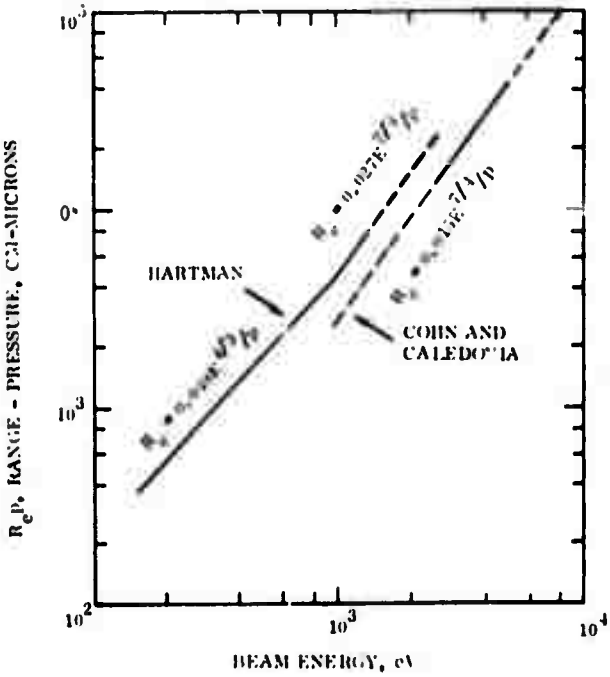

(B)

Figure 4. (A) Measurements[2] of electron beam energy required for 34 inch range versus pressure. (B) Power law fits to the data of Hartman[2] and Cohn and Caledonia.[6] The solid curves show the range of the experimental data. Dashed portions are extrapolations from the data.

determine a range relation based on N_2 first negative emission data over the energy range from 2 to 5 kilovolts; a power law fit to their data yields

$$R_e = 0.015\ E^{7/4}/p \qquad 2500 \leq E \leq 5000 \tag{5}$$

Equation (5) is plotted in Figure 4B. Both sets of data[2,6] have the same dependence for energies above 1000 electron volts; however, they are shifted by a factor of 1.8. Since Cohn & Caledonia measured the energy deposition directly, we tend to favor their results. Figure 5 shows the electron beam energy plotted as a function of pressure for several ranges, using Equation (5). The minimum electron beam range would be twice the length of the tank (between 2 and 4 meters). At 10 microns pressure, the beam energy would be less than 1 keV rising at 100 microns to about 4 keV.

Ionizing collisions producing electron-ion pairs is the major process transferring energy from the electron beam to the gas. Subsequently chemical processes are initiated by both the ion and secondary electron. The secondary electrons must come to rest in the gas. This can be accomplished by confining the electrons with a 10 gauss axial magnetic field or by maintaining sufficient pressure to keep the secondary electron range short which would place an additional limitation on the lowest operating pressure that could be used for the laboratory experiment. The range of the secondary electrons, R_{se}, is

$$R_{se} \approx (1/p) \text{ meter}$$

where p is the pressure in microns of Hg. Note that at 1 micron pressure, a 1 meter secondary electron range would be larger than a 50 cm tank and comparable to a 150 cm tank, while at 10 microns the 10 cm range would be significantly smaller than the tank dimensions. Thus, it is recommended that (with no magnetic field) 10 microns be the lowest operating pressure for careful analysis of the data, although considerable information could be derived from lower pressure data.

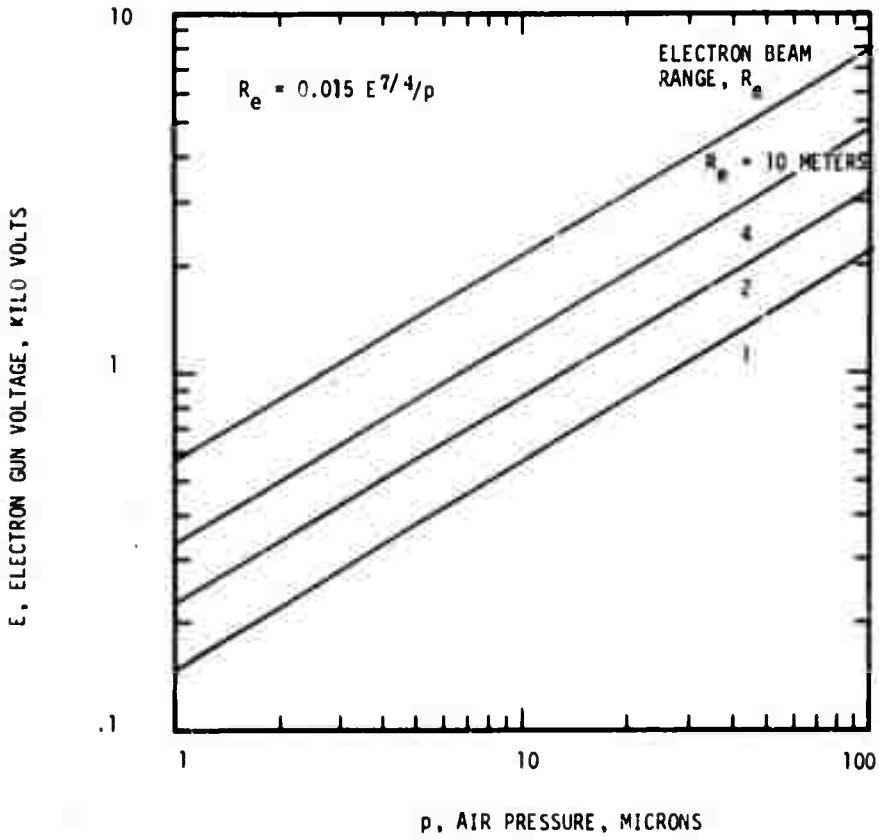

Figure 5. Electron beam voltage as a function of pressure for 1, 2, 4, and 10 meters range, based on the data of Cohn & Caledonia.[6]

Electron Beam Excited Air Chemistry

The primary interaction of the electron beam with air is the formation of ion-electron pairs. A fast electron loses about 35 eV for each ion-electron pair it produces. The cross section for nitrogen ionization is shown in Figure 6 as a function of the electron energy. The N_2^+ ion is produced mainly in the ground state with some production of excited states. Figure 6 also presents the cross section for excitation of the $N_2^+(B)$ state.[7] The $N_2^+(B)$ state radiates (7×10^{-8} second lifetime) in the N_2^+ first negative system. From a detailed spectral analysis of this radiation one can determine the gas density, gas temperature, and N_2

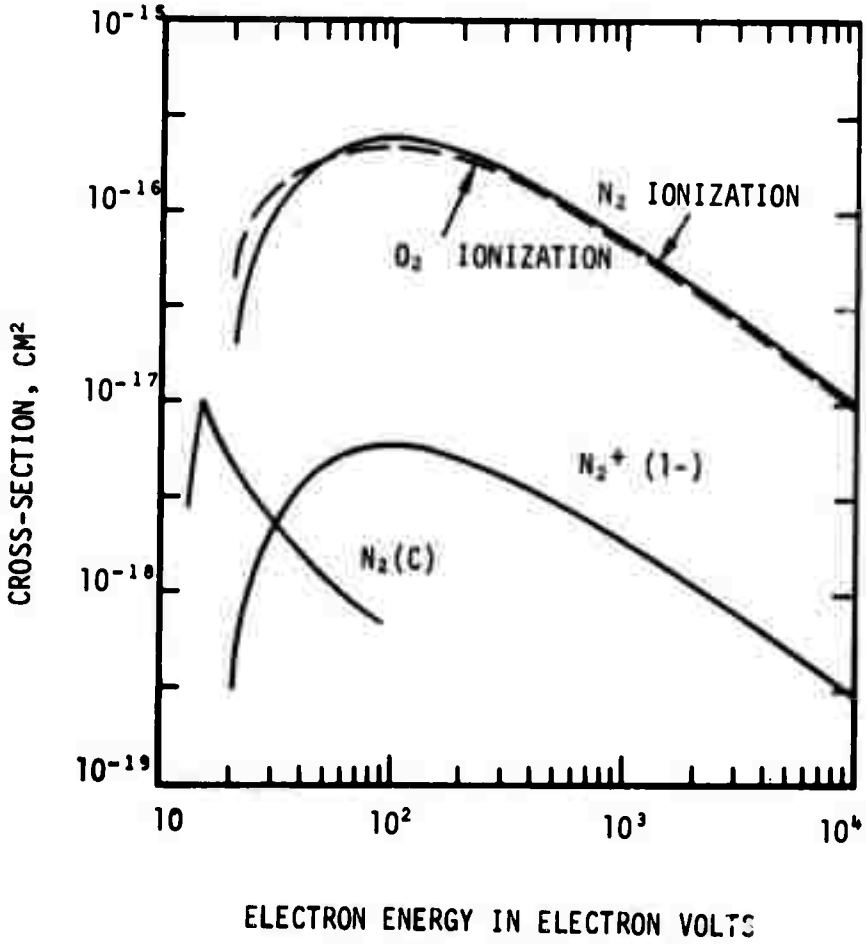

Figure 6. The cross section for ionization of nitrogen and oxygen by electrons. The cross section for excitation of the N_2^+ [B] (1st negative) and N_2[C] (2nd positive) states.

vibrational excitation.[8] The cross section for O_2 ionization by electrons is comparable to that of N_2 (see Figure 6).

The secondary electrons also produce some ionization and excitation as they collisionally thermalize starting from an initial translational energy. An example of an important excitation process by the secondary electron is the formation of the $N_2(C)$ state; the cross section, which peaks around 15 eV, is also shown in Figure 6.[9] $N_2(C)$ state production is important as it quickly radiates (through the 2+ and 1+ bands) and forms the long life $N_2(A)$ metastable state.

Fast and slow chemical reactions take place in the gas. Initially, the excited electronic states radiate. Figure 7 shows the ultraviolet and visible air spectra obtained by Hartman.[2]

The fastest chemistry is in ionic reactions (rates at room temperature).

$$N_2^+ + O_2 \rightarrow N_2 + O_2^+ \qquad 3\times10^{-10}\,\text{cc/sec} \tag{6}$$

$$N_2^+ + e \rightarrow N(^2D) + N \qquad 2.8\times10^{-7} \tag{7}$$

$$O_2^+ + e \rightarrow \begin{cases} O(^3P) + O(^1D) & 2.2 \times 10^{-7} \\ O(^3P) + O(^1S) & 2.1 \times 10^{-8} \end{cases} \tag{8}$$

The following slow reactions can be neglected

$$\left.\begin{matrix} N_2^+ + O_2 \\ N_2 + O_2^+ \end{matrix}\right\} \rightarrow NO + NO^+ < 10^{-17}$$

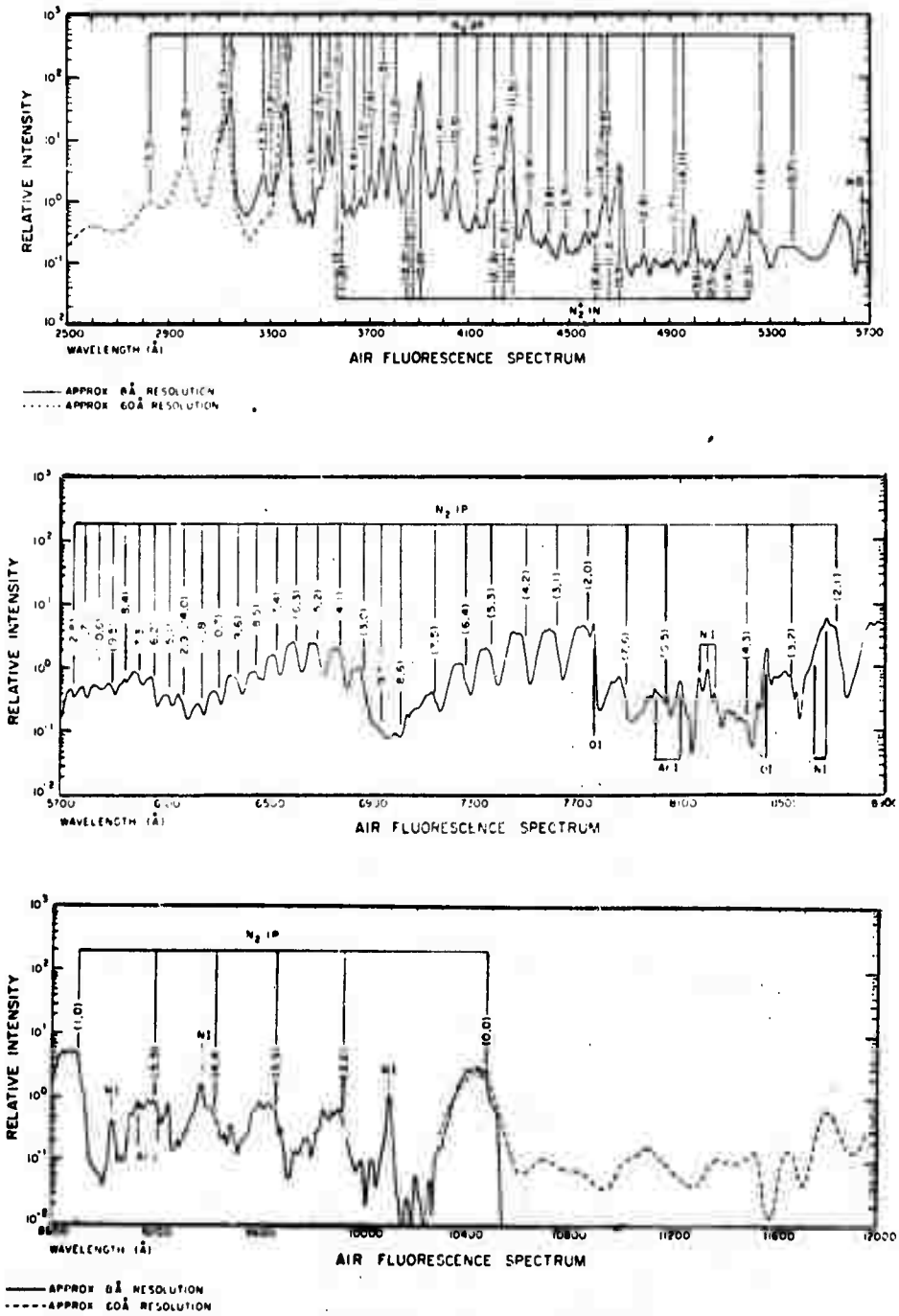

Figure 7 The electron excited luminescent spectrum of air at 70 microns pressure. Electron energy is 850 eV. Data of Hartman.[2]

After the atom concentrations build up to an appreciable level, they, too, perform important chemical reactions which lead to other species.

$$N + O_2^+ \rightarrow NO^+ + O \qquad 1.8 \times 10^{-10} \qquad (9)$$

$$\left.\begin{matrix} O_2^+ \\ N_2^+ \\ O^+ \end{matrix}\right\} + NO \rightarrow NO^+ + \left\{\begin{matrix} O_2 & 8 \times 10^{-10} \\ N_2 & 5 \times 10^{-10} \\ O & 2 \times 10^{-12} \end{matrix}\right. \qquad (10)$$

$$NO^+ + e \rightarrow \left\{\begin{matrix} N + O & 1 \times 10^{-7} \\ N(^2D) + O(^3P) & 3 \times 10^{-7} \end{matrix}\right. \qquad (11)$$

$$O + N_2^+ \rightarrow \left\{\begin{matrix} NO^+ + N(^2D) & 1 \times 10^{-11} \\ NO^+ + N & 2.5 \times 10^{-10} \\ N_2 + O^+ & 1 \times 10^{-12} \end{matrix}\right. \qquad (12)$$

$$N_2 + O^+ \rightarrow NO^+ + N \qquad 1 \times 10^{-12} \qquad (13)$$

$$O_2 + O^+ \rightarrow O + O_2^+ \qquad 2 \times 10^{-11} \qquad (14)$$

$$N^+ + O_2 \rightarrow \left\{\begin{matrix} N + O_2^+ & 6\times10^{-10} \\ NO + O^+ & 1\times10^{-12} \\ NO^+ + O & 3\times10^{-10} \end{matrix}\right.$$

$$N + NO \rightarrow \left\{\begin{matrix} N_2^+ + O & 3\times10^{-12} \\ N_2 + O^+ & 1\times10^{-12} \\ N + NO^+ & 9\times10^{-10} \end{matrix}\right.$$

$$N^+ + O \rightarrow N + O^+ \qquad 1\times10^{-12}$$

Through this sequence of reactions several energy sources are now available to produce infrared radiation. The main chemical reactions are

$N + NO \rightarrow N_2 + O$	2.5×10^{-11} cc/sec	(15)
$N + O_2 \rightarrow NO + O$	$\begin{cases} 1.1 \times 10^{-16} \\ 1.4 \times 10^{-11} \exp(-3600°K/T) \end{cases}$	(16)
$N + O_2(a'\Delta_g) \rightarrow NO + O$	3×10^{-15}	(17)
$N(^2D) + O_2 \rightarrow NO + O$	6×10^{-12}	(18)
$O + O_2 + (M) \rightarrow O_3^* + (M)$	6×10^{-34} cc^2/sec	(19)
$O + NO + (M) \rightarrow NO_2^* + (M)$	8×10^{-32} cc^2/sec	(20)
$O + NO \rightarrow NO_2^* + h\nu$	7×10^{-17} cc/sec	(21)
$O + O_3 \rightarrow O_2 + O_2$	6×10^{-15}	(22)
$O + NO_2 \rightarrow NO + O_2$	6×10^{-12}	(23)

where (M) is a colliding third body. Reactions 10, 12, 13 and 16 through 21 can produce vibrational excitation in the radiating species NO^+, NO, O_3, and NO_2.

Vibrationally excited nitrogen is produced in collisions with secondary electrons. Between 5 and 10% of the total beam energy goes into exciting N_2 vibration. This energy can transfer to CO, H_2O, and CO_2 vibrational modes which are infrared active. The main transfer processes are illustrated in Figure 8.

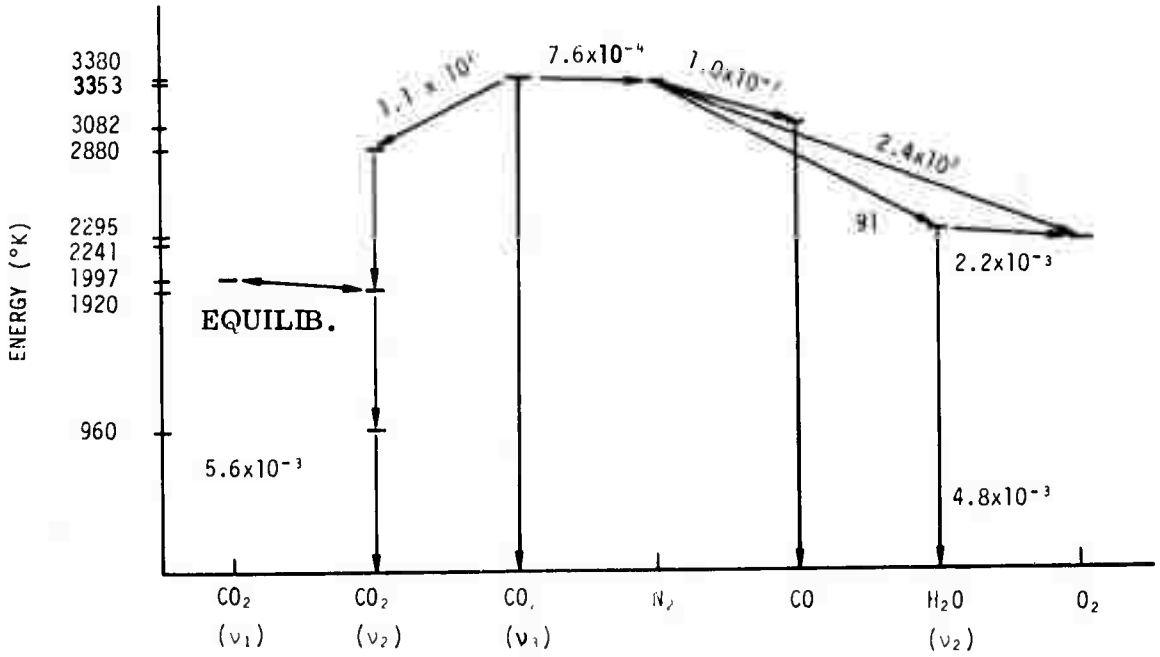

Figure 8. Vibrational energy diagram for CO_2, N_2, CO, H_2O, and O_2. The solid vertical lines are permitted radiative transitions. The arrows between states are the times for deactivation or vibration transfer for air at 100 microns pressure and at room temperature.

The fastest three-body reactions are those involving ions, in particular, those which form negative ions by electron attachment. The main reaction is

$$e + O_2 + O_2 \rightarrow O_2^- + O_2 \qquad 1.34 \times 10^{-30}\ cc^2/sec$$

In a gas containing only $N_2 + O_2$, the electrons are attached to O_2^- by this reaction. However, with the addition of atoms and ozone, further reactions take place.

$$O_2^- + O \rightarrow O_2 + O^- \qquad 1 \times 10^{-10}$$

$$O_2^- + O_3 \rightarrow O_2 + O_3^- \qquad 4 \times 10^{-10}$$

$$O_2^- + NO \rightarrow O + NO_2^- \qquad 1 \times 10^{-11}$$

$$O_3^- + O \quad O_2 + O_2^- \qquad 1 \times 10^{-10}$$

An important feature of negative ion chemistry are the reactions that release the electrons

$$O_2^- + N \rightarrow NO_2 + e \qquad 4 \times 10^{-10}$$

$$O^- + O \rightarrow O_2 + e \qquad 2 \times 10^{-10}$$

$$O_2^- + O \rightarrow O_3 + e \qquad 3 \times 10^{-10}$$

$$O_3^- + O \rightarrow 2O_2 + e \qquad \sim 10^{-10}$$

Thus, cyclic reactions can maintain high electron concentrations when sufficient atomic oxygen is available. At a pressure of 100 microns, the O_2^- formation rate is about 2 seconds, which is longer than the time to diffuse to the walls where neutralization takes place. In addition, atomic oxygen can release electrons. At an electron beam current of 10 milliampere the steady state electron concentration is 10 times the negative ion concentration. This factor is proportional to electron beam current. That is, there would be a larger fraction of electrons at higher currents. For lower current, the experiment must be run at lower air pressures in order to keep the negative ion concentrations small.

Because of the large number of reactions, computer programming of the kinetics of this reaction would be required to give exact predictions of the infrared emission from these bands. In the next section of this paper estimates are presented which are adequate for experiment planning.

2.2 Measurement of Gas Temperature, Density, and Species

Electron beam excitation of nitrogen produces intense $N_2^+(1-)$ emission spectrum which is dependent on the gas temperature. The electron excited air spectra is shown in Figure 7. $N_2(1-)$ bands have large vibrational spacing and are free from other contaminating spectra. Figure 9 shows the detailed (0,0) band rotational temperature spectra at room temperature.[10] The use of this spectrum for temperature determination has been studied extensively and shown to furnish temperatures to a few degrees accuracy.[10] The nitrogen vibrational temperature can be obtained from band intensity ratios of the (0,1), (0,2), (1,2), and (2,4) bands.[8] O'Neil's curves are shown in Figure 10.[8] This method for determining the vibrational temperature is sensitive only above about 900°K.

2.3 Circulation Effects in the Tank

There would be several heat sources and sinks in the tank which would tend to set up convection currents. The electron beam would heat the gas along the path of the beam. Cold surfaces (near liquid nitrogen temperature) required by the infrared system would cool the gas near these surfaces. Temperature dependent chemistry would require knowledge of the gas temperature. Fortunately, temperature profiles could be obtained from an analysis of the $N_2^+(1-)$ spectrum excited by the electron beam. An estimate of the amount of convection could be determined from measurements of temperature profiles in the tank.

Convection would tend to reduce temperature differences in the tank by bringing the gas into contact with the wall more frequently. However, this would introduce a more serious effect of transporting active species to the wall more rapidly. The problem of heat convection will be discussed in more detail in the next section where details of the experimental arrangement are treated.

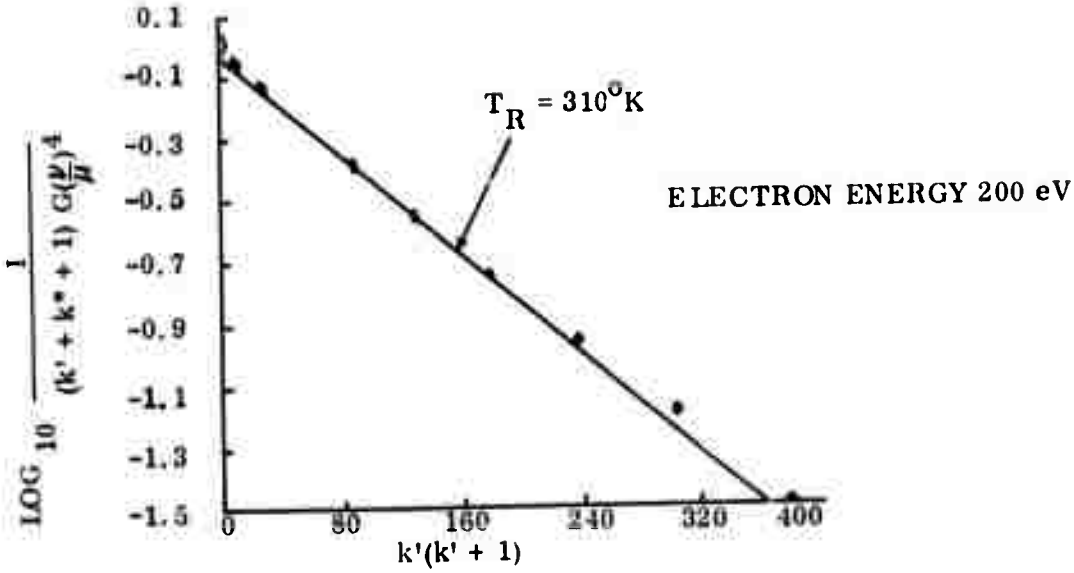

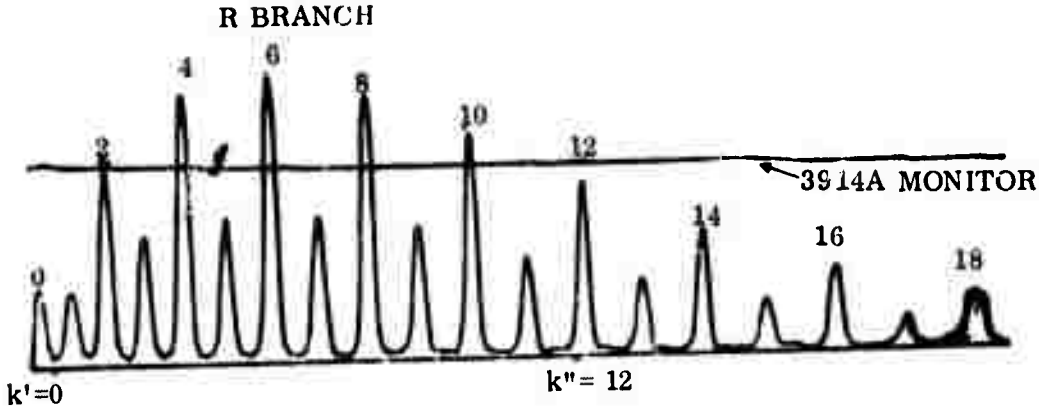

Figure 9. The rotation spectrum of the $N_2^+(1-)$ ($v'=0$, $v''=0$) transition around the line center of 3914A.[10] An analysis which determines those rotational temperatures, equal to the translational temperature is also shown in this experiment.

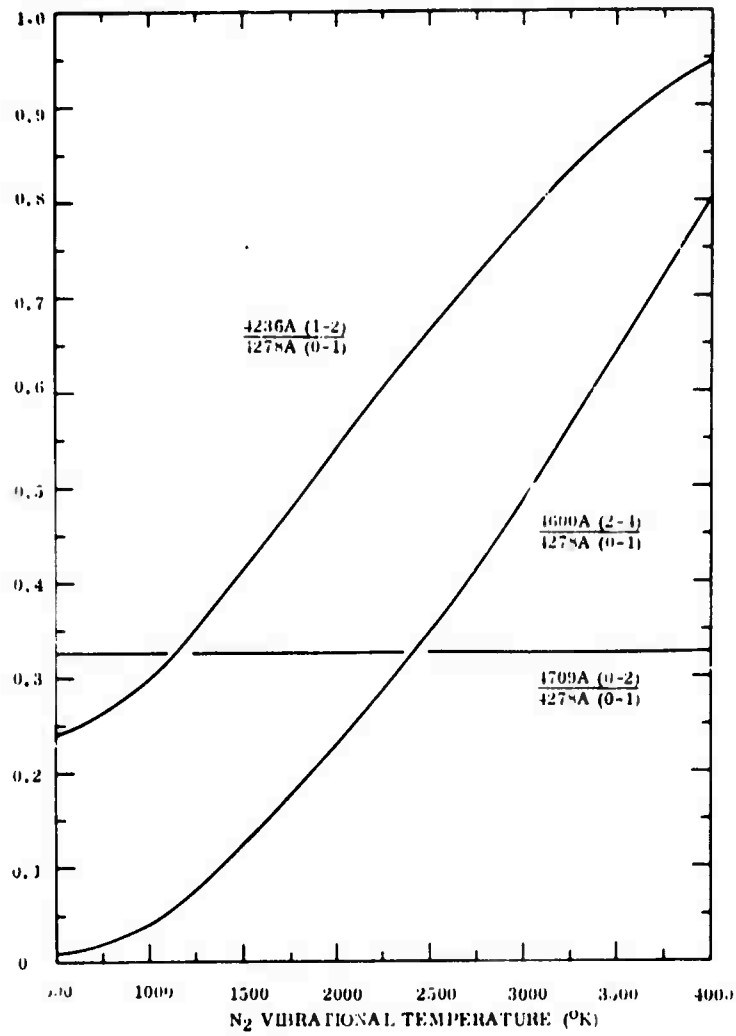

Figure 10. The ratio of the intensities of vibration bands transitions of the N_2^+ [1-] system versus the N_2 vibrational temperature.[8] The sensitivity becomes linear above about 900 °K.

Section 3

EXPERIMENTAL APPARATUS

A schematic of the experimental apparatus is shown in Figure 11. A 1 meter diameter and 1.5 meter long tank would contain the air. An electron beam having energies ranging from 300 to 2000 eV, depending on pressure, would be directed along the axis of the tank. An electron gun would be located near the top of the tank. Infrared and visible emission from the gas would be observed with the usual detectors. For the 8 to 30 micron region, an infrared detector would be cooled to liquid helium temperatures, and the optics would also require cooling, possibly down to liquid nitrogen temperature. Cooled baffles should also be used: (1) to reduce the thermal radiation illuminating the surfaces of the optical elements, and (2) to minimize the convection currents generated by the cooled surfaces. A cooled mirror would be placed on the side of the tank opposite to the detector.

In order to minimize the convection currents caused by the cold optics, the infrared detector would be located at the bottom of the tank and the cold mirror at the top. At the cooled optical components on the bottom, the higher density cooled gas would be thermally trapped and thus would not induce circulation in the tank. At the cooled surface at the top of the tank, a suitable set of baffles with counterflows would be required to minimize convection currents.

Two types of infrared optics could be considered, which are trade-offs between better optical resolution with the optical system and the reflecting mirror focus on the axis of the tank (see Figure 12A) and better aerodynamic baffling with the optical system focused on the reflecting mirror (see Figure 12B). In case shown in Figure 12B, the aperture in the mirror baffles could be small and the air cooled by the surface simply isolated with a small counterflow (see Figure 12C).

The gas would be heated by the electron beam along the tank axis which would produce circulation currents, raising the air at the center to the top. This effect is treated in detail in a later section.

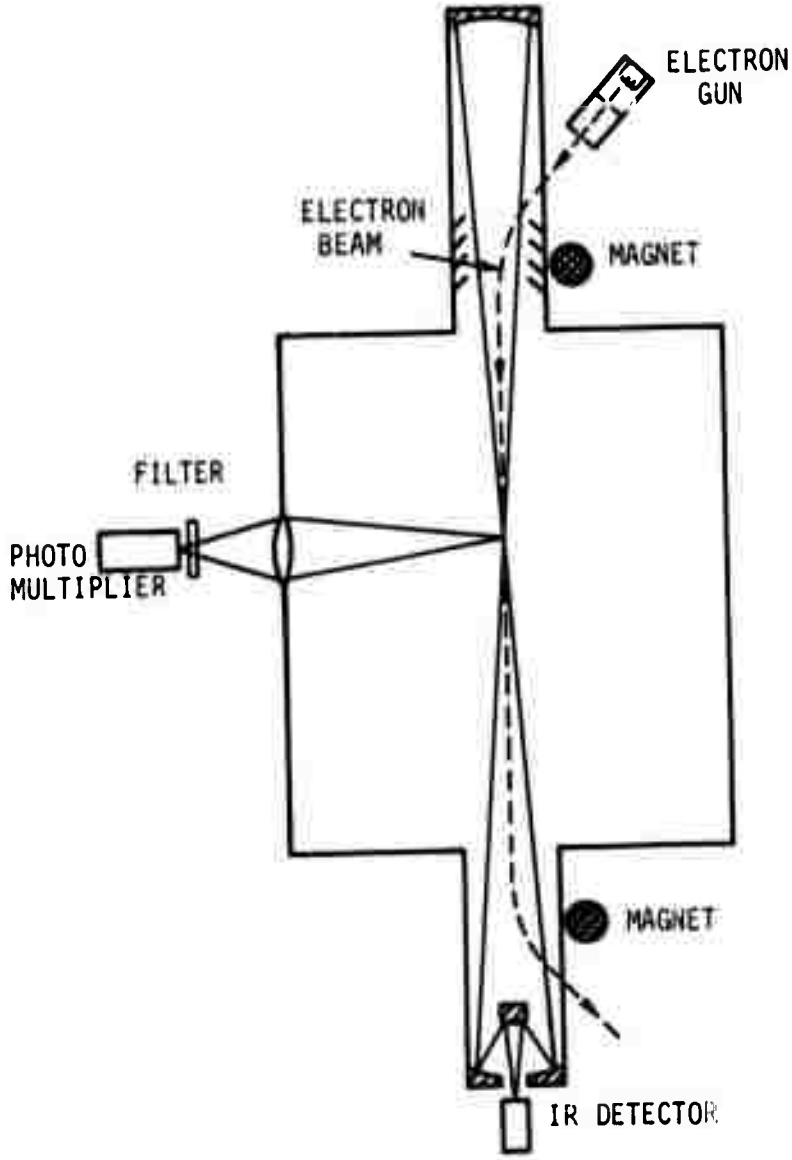

Figure 11. Schematic of experimental arrangement for measuring the ultraviolet, visible and infrared emission from gas excited by an electron beam.

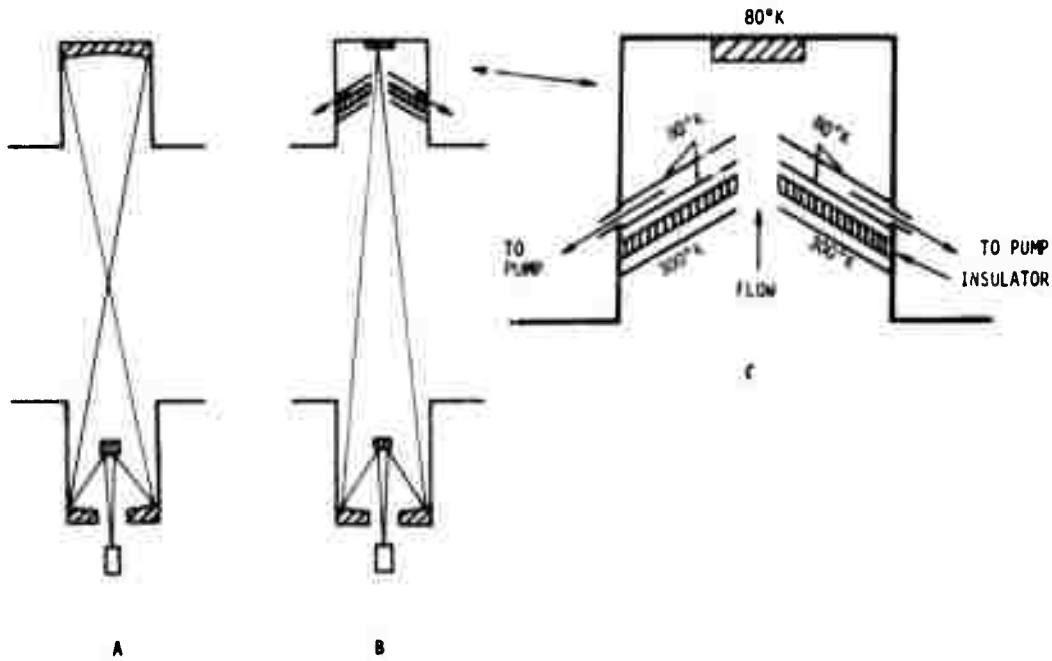

Figure 12. Several arrangements of the infrared optical system. (A) is for good focusing at the center of the tank; (B) is for focusing at the opposite wall so that a flow system can be used with a cool surface; (C) give details of the flow.

Visible light measurements of direct electron beam excitation or of chemical recombination would be made with filter/photomultiplier systems. More detailed spectral information could be obtained with spectrometers. This radiation could be observed through windows placed on the side of the tank. N_2 rotational and vibrational temperature could be determined by the electron excited radiation.

Other types of measurements could be made. For example, ionic species could be observed with a mass spectrometer. Neutral species could be determined by laser scattering techniques.

A major feature of this experiment is that the electron beam current could be varied over many orders of magnitude from microamperes to tens of milliamperes. This would permit the production of significant densities of reaction products at high power levels, but only trace quantities at lower levels. Of course,

those products removed by wall collisions would live only the characteristic time of the apparatus, of the order of 0.1 to 1 second. By varying the excitation level in the tank, one could vary the composition of the excited species, and different processes could be studied. At the high power levels, many electrons and ions would be produced, and ion-electron recombination would dominate the air chemistry. At low currents, the reactions with neutral species would dominate.

The electron beam current would be modulated on/off for periods of several seconds. By measuring both phase and intensities, one could distinguish between infrared radiation induced by direct electron excitation and infrared radiation following chemical reactions.

3.1 Chemistry Produced by the Electron Beam

The ionization production by the electron beam is given by the relation

$$\frac{dn^+}{dt} = I \sigma [M] \tag{24}$$

where n^+ is the number of ion-electron pairs produced per cm by the electron beam; I is the beam current; σ is the ionization cross section (see Figure 6); and $[M]$ is the number density of air molecules. The ionized and excited species produced by the beam at the center of the tank would tend to diffuse to the wall with a characteristic diffusion time (see Figure 3), which the concentrations of those species that are removed by the wall would reach at steady state levels. (On the other hand, the concentrations of the species not removed in collisions with the wall, such as NO, would increase.) Ions would neutralize at the wall and atoms would recombine. For the case of negligible gas neutralization, the steady state level can be calculated by averaging the ionization over the area of the tank for the diffusion time.

$$[M^+]_o = \left(\frac{dn^+}{dt}\right) t_w / A_t = I \sigma [M] t_w / A_t \tag{25}$$

$[M^+]_0$ is the steady state ion concentration without gas neutralization; t_w is the diffusion time to the wall; and A_t is the cross sectional area of the tank. For example, consider air at p = 10 microns for which $t_w = 0.15$ seconds and $[M] = 3.2 \times 10^{14}$ per cm^3. Let I = 10 milliamperes, $\sigma = 3 \times 10^{-16}$ cm^2, and $A_t = 8 \times 10^3$ cm^3. The fraction of the gas ionized by the electron beam during this diffusion time becomes:

$$[M^+]_0 / [M] = I \sigma t_w / A_t = 3.5 \times 10^{-4} \tag{26}$$

The ion density becomes

$$[M^+]_0 = 3.5 \times 10^{-4} [M] = 1.1 \times 10^{11}/cc \tag{27}$$

This is a large overestimation of the ionization level because ions and electrons recombine through Reactions (7), (8), and (11). The steady state ion concentration is at a lower level

$$[M^+] = \sqrt{I\sigma[M]/A_t k_r} = \sqrt{[M^+]_0 / k_r t_w}$$

where k_r is the average air recombination rate constant for Reactions (7), (8), and (11). For the example above, using $k_r = 3 \times 10^{-7}$ cm^3/sec, $t_w = 0.15$ sec and $[M^+]_0 = 1.1 \times 10^{11}$ we obtain

$$[M^+] = 1.6 \times 10^9/cc$$

The time to reach this steady state level is approximately $\sqrt{1/k_r[M^+]}$ which is 0.045 seconds for this example.

Gas Heating by the Electron Beam

To estimate the temperature rise of the gas produced by the electron beam, we assume that the thermal energy input to the air is furnished by 2/3 of the electron beam energy deposited in the gas. The air temperature rise, ΔT, becomes

$$\Delta T = (2/3)(35\text{eV})I\sigma t_w/3.5kA_t \tag{28}$$

$$= (2/3)(35)\ ([M^+]_0/[M])(1.16 \times 10^4/3.5)\ ^oK$$

$$= 8 \times 10^4\ [M_0^+]/[M])\quad ^\circ K$$

$$= 8 \times 10^4\ (I\ \sigma\ t_w/A_t)\quad ^\circ K$$

For $t_w = 0.15$ sec, $\Delta T = (3\ I)\ ^\circ K$ for the current I in milliamperes. Thus, $\Delta T = 30\ ^\circ K$ for 10 milliamperes.

Thermal Convection

The main heating source would be from the electron beam. The beam would irradiate the gas at the center of the tank, with the heating being proportional to the beam current and nearly independent of the gas pressure. On the other hand, the transport of this heat to the walls either by laminar diffusion or by convection would be pressure dependent. Laminar diffusion was previously discussed and steady state temperatures and diffusion times derived.

Convective cooling would be produced by gravitational forces. While the heated central region would have a lower density tending to rise, circulation would be retarded by viscous drag on the outer wall. Flow patterns for both vertical and horizontal beams are illustrated in Figure 13. The electron beam heating rate is

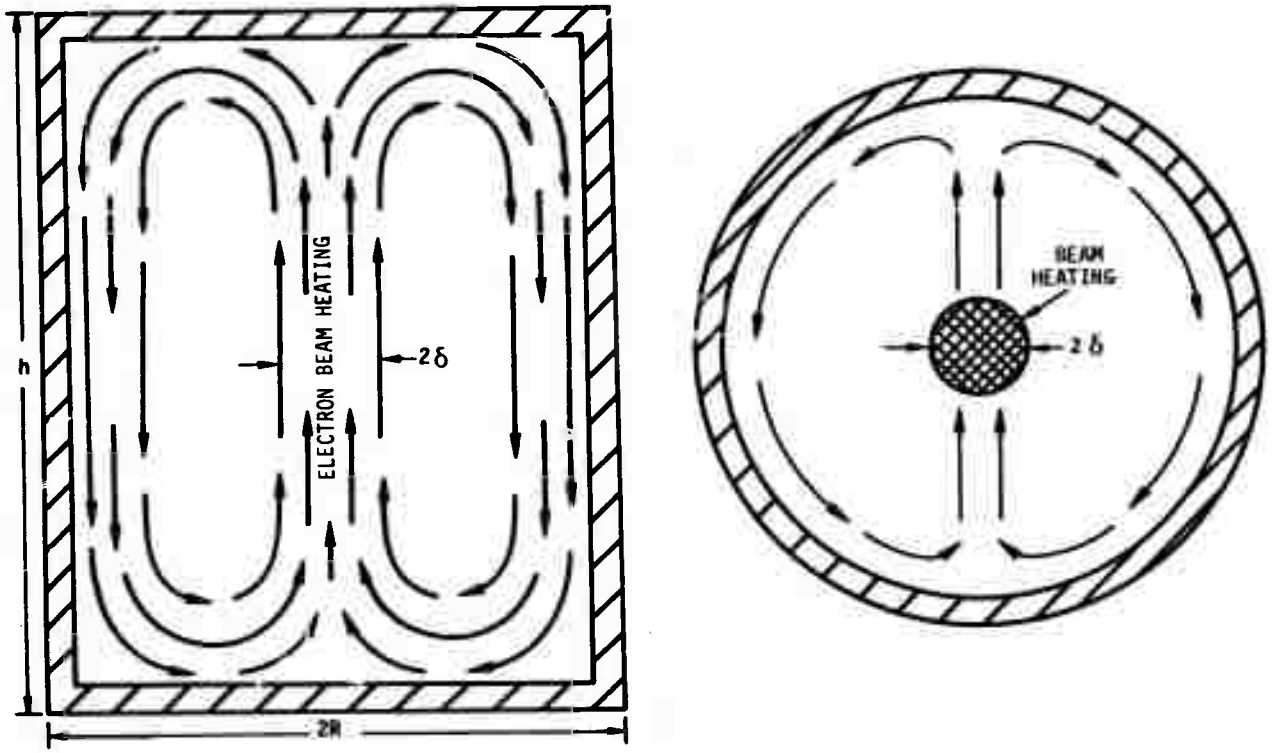

Figure 13. Thermal convective patterns with electron beam heating. The beam is confined to a core along the axis of the tank and is directed vertically or horizontally.

$$dQ/dt = [M]\,\sigma I \varepsilon \tag{29}$$

where [M] is the number density, σ is the cross section for ionization (see Figure 6), I is the electron beam current, and ϵ, the energy transferred into translation per ion pair, depends on time and pressure. We shall use 2/3 of the energy required per ion-electron pair; thus, ϵ = 24 electron-volts per ion-pair. The gas temperature rise ΔT as a function of an energy input ΔQ is determined from the relation

$$\Delta Q = \pi\,\delta^2\,\rho\,C_p\,T(\Delta T/T) \tag{30}$$

where δ is the radius of the heated central core; ρ, the density; C_p, the specific heat; and T, the temperature. At constant pressure

$$-\frac{\Delta\rho}{\rho} = \frac{\Delta T}{T} = \frac{(\Delta Q)}{\pi\,\delta^2\,\rho\,C_p\,T} = \frac{(\Delta Q)(\gamma-1)}{\pi\,\delta^2\,\gamma p} \tag{31}$$

The buoyancy force is

$$g\,\Delta\rho(\pi\,\delta^2 h) = g\rho\,\frac{(\Delta Q)(\gamma-1)h}{\gamma\,p} \tag{32}$$

where h is the length of the tank, g is the gravitational constant, and γ is the ratio of specific heats.

The buoyancy force is produced by the difference in density along a vertical column. In the case of a horizontal electron beam the center of the tank is heated. Since the gas above the core is colder, there is thus a buoyancy force tending to raise the central region; see Equation (32). Since for a vertical electron beam, the gas can be heated nearly uniformly along a vertical column, the buoyancy

force does not exist except for horizontal flow into the core region. There radial mixing would produce some buoyancy force, but not so much as in the case of the horizontal beam. Thus, a system using a vertical electron beam would minimize convective heat transfer. To further minimize convection the electron gun could be placed at the top of the tank and with the electron beam pointing down. The heating density would be higher near the electron gun and the gas would get hotter at the top. This would add to the stability against convective current formation.

We will now treat the horizontal beam case and compare magnitudes of the convective and conductive heat transfer. The shear force on the tank is

$$\mu(dV/dy)(2\pi Rh) = 2\pi h\lambda\rho c\ V \tag{33}$$

where $(2\pi Rh)$ is the tank area; $\mu = \rho c\lambda/3$ is the viscosity, λ is the mean-free-path for collision and c is the gas thermal velocity. For the velocity gradient we used $dV/dy \approx 3V/R$. At the pressure near the crossover from conduction to convection, the heat is quickly distributed, keeping the density and temperature gradients small. The heated core quickly spreads radially to about R/3 and the gradients near the wall are thick. Equating forces

$$g\ \rho\ \frac{(\Delta Q)(\gamma-1)h}{\gamma\ p} = V\ \rho\ c\ \lambda\ 2\pi\ h \tag{34}$$

(ΔQ) is the average gas heating over the time a molecule remains in the beam. $\Delta Q = (dQ/dt)\ \delta/V = M\ I\sigma\epsilon\delta/V$. Substituting for ΔQ and solving for V^2,

$$V^2 = \frac{(\gamma-1)g(I\sigma\varepsilon)\delta[M]}{2\ \pi\ \gamma\ p\ c\ \lambda} \tag{35}$$

The convection time $\tau_{con} \equiv 2R/V$ becomes

$$\tau_{con} = 2R \sqrt{\frac{2\pi \gamma \ pc\lambda}{(\gamma-1)(I\sigma\varepsilon)g[M]\delta}} \tag{36}$$

τ_{con}, plotted as a function of pressure for several current values is shown in Figure 14. The diffusion cooling time is proportional to pressure. For convection, however, cooling time varies inversely with the square root of the pressure. In addition, higher electron beam currents decrease the convection cooling time. The smaller of the times shown in Figure 14 should be used.

The simple analysis for convective heat transfer assumes a Reynolds number, high enough that diffusion effects can be neglected. This analysis is only appropriate at high pressures far from the diffusion curves intersection. The region where this simple analysis is not applicable is indicated by dashed lines in Figure 14. Note that diffusion cooling dominates up to pressures of about 0.1 Torr even for high currents. Thus, up to this pressure one can use a simple analysis considering only diffusion to the wall and neglecting convection flows.

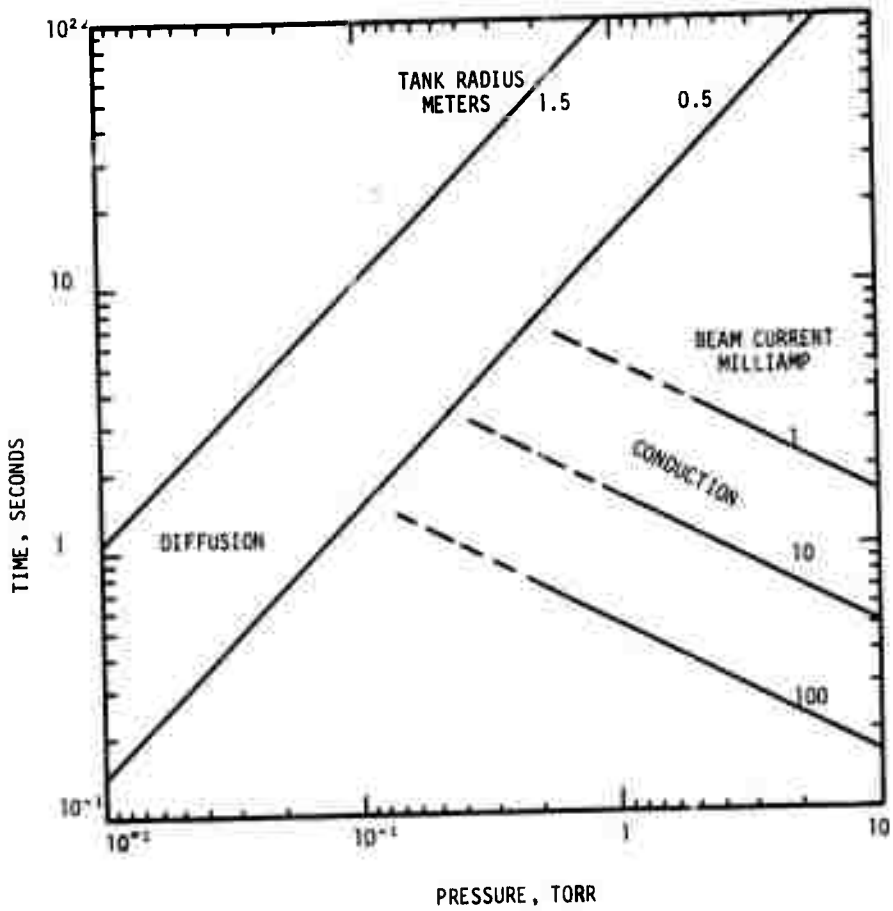

Figure 14. The time for thermal conduction and convection losses to the wall as a function of the gas pressure in torr. The tank radius is 0.5 and 1.5 meters. The beam current is 1, 10 and 100 milliamperes. The solid portion of the convection curve apply to both tank sizes, while the dashed portion applies to the 1.5 meter radius. The curves end where the analysis presented does not apply.

Section 4

INFRARED EMISSION FROM THE GAS

The major sources of infrared-excitation energy are: (1) the direct excitation of N_2 vibration by the secondary electrons, and (2) chemical reactions involving atoms. Atomic nitrogen and oxygen result from the dissociative recombination Reactions (7), (8), and (11) with each ion-electron pair yielding two atoms. The ratio of N to O atoms depends on the electron current level and the running time. The latter is related to the growing levels of NO and O, which may not react with the wall. The major reactions producing infrared active species are Reactions (12) and (16) to (21); however, the vibrational distributions of the reaction products are uncertain.

Additional radiation is produced by vibration transfer from N_2 to CO_2, H_2O, and OH, etc. CO_2 produces infrared radiation at 15, 10, 4.3, and 2.9 microns and at shorter wavelengths. Most of the CO_2 radiation would be emitted in the 4.3 micron band. However, CO_2 10- and 15-micron radiation regions could also be major sources. H_2O vibration radiates in the 6.5 and 2.7 micron regions and shorter wavelengths while, at room temperature, H_2O rotation bands radiate at 20 micron and longer wavelengths, extending below 10 microns at elevated temperatures.

We will now estimate the infrared radiation from vibrational energy. We assume that 6% of the energy deposited in the air by the electron beam goes into nitrogen vibrational energy. Hence, at 35 eV per ion-electron pair, 2 eV goes into vibration. Since each vibrational quantum has approximately 0.3 eV energy, approximately 7 vibrational quanta are produced per ion pair. Using Equation (24), the nitrogen vibrational excitation becomes:

$$(dn^*_{N_2}/dt) = 7\ (dn^+/dt) = 7\ I\ \sigma\ [M] \tag{37}$$

Preceding page blank

where $n^*_{N_2}$ is the number of vibrationally excited N_2 produced per cm path of the electron beam. For a 10 milliampere beam and 10 microns air pressure, the production rate for N_2 vibration becomes

$$(dn^*_{N_2}/dt) = 7\ (6 \times 10^{16})\ (3 \times 10^{-16})\ (3.2 \times 10^{14}) \tag{38}$$

N_2 vibrational excitation can transfer to other molecules or be deactivated at the wall. At 10 microns pressure, nitrogen migrates to the wall in about 0.15 seconds with only a small fraction of vibrational excitation transfer to other molecules. We shall consider the two extreme cases where: (1) the wall is fully catalytic and (2) the wall is noncatalytic to N_2 vibration. We assume that the main vibrational transfer to infrared active species is by the reaction

$$N_2^* + CO_2 \rightarrow N_2 + CO_2\ (001) \qquad k_c = 4 \times 10^{-13}\ cm^3/sec \tag{39}$$

<u>Case I: Fully Catalytic Wall</u>.

The steady state fractional vibrational population becomes

$$[N_2^*]\ /\ [N_2] = 7\ [M^+]_0\ /\ [M] = 7\ \sigma\ I\ t_w\ /\ A_t \tag{40}$$

For 10 milliamps and $t_w = 0.15$ sec, $[N_2^*]/[N_2]$ becomes 2.4×10^{-3}. The estimated time to deplete the N_2^* by reaction (39) is

$$N_2^* \text{ depletion time} \equiv - [N_2^*] / (d[N_2^*] / dt) = 1/k_c [CO_2] \tag{41}$$

$$= 2.5 \times 10^{12} / [CO_2]$$

where $[CO_2]$ is the number density of CO_2. In Equation (39) it is implicitly assumed that the energy transferred to CO_2 is removed rapidly; that is, the CO(001) concentration remains small so that the reverse reaction $CO_2(001) + N_2 \rightarrow CO_2 + N_2^*$ can be neglected. The main loss of energy from $CO_2(001)$ is through 4.3 micron radiation with a radiative lifetime of 0.003 seconds. The time, τ_{equ}, for the CO(001) to reach equilibrium through Reaction (39) is

$$\tau_{equ} \equiv ([N_2^*] / [N_2]) / (d[CO(001)] / [CO_2]\, dt) = 1/k_c [N_2] \tag{42}$$

$$\tau_{equ} = 1/(4 \times 10^{-13})(3.2 \times 10^{13} p) = (0.08/p) \text{ seconds}$$

where p is the air pressure in microns. Note that at p = 30 microns, $\tau_{equ} = \tau_{4.7\mu} =$ 0.003 seconds, the $CO_2(001)$ radiative lifetime. Thus, Equation (41) is valid only for p < 30 microns. For pressures above 30 microns, the $CO_2(001)$ state maintains an equilibrium population and the N_2 vibrational depopulation is controlled by 4.3μ emission. The rate controlling relation is

$$- \frac{dN_2^*}{dt} = \frac{[CO_2(001)]_{equ}}{\tau_{4.7}} = [CO_2]\,[N_2^*] / [N_2]\,\tau_{4.7} \tag{43}$$

The N_2^* depletion time becomes

$$- [N_2^*] / (d[N_2^*] / dt) = \tau_{4.7} ([N_2] / [CO_2]) \tag{44}$$

$$= (0.003)(.8)/\phi_{CO_2}$$

$$= 0.0024/\phi_{CO_2} \text{ seconds}$$

where ϕ_{CO_2} is the mole fraction of CO_2. Using the natural atmospheric concentration $\phi_{CO_2} = 3.4 \times 10^{-4}$, the N_2^* depletion time is 7 seconds. For $\phi_{CO_2} = 10^{-2}$, the N_2^* depletion time is 0.24 seconds.

The N_2^* depletion time is compared to the diffusion time to the wall in Figure 15. Note that these times cross at 25 microns and 500 microns for 1% and 0.034% CO_2 mole fraction, respectively. In the case of the fully catalytic wall the N_2^* depletion time is determined by the shorter time shown in Figure 15. That is, the depletion time is determined by wall losses at low pressures and transfer to CO_2 at high pressures.

Case II: Non-Catalytic Wall

In this case the nitrogen vibrational population continues to increase until balanced by transfer to CO_2 through Reaction (39). The depletion times are given by the CO_2 curves in Figure 15.

The 4.3 micron CO_2 radiation intensity in the equilibrium region ($p > 30$ microns) is

$$I_{4.3\mu} = \frac{[CO_2(001)]}{\tau_{4.7}} = 330\ [CO_2]([N_2^*] / [N_2]) \frac{\text{Photons}}{\text{cm}^3\text{-sec}} \tag{45}$$

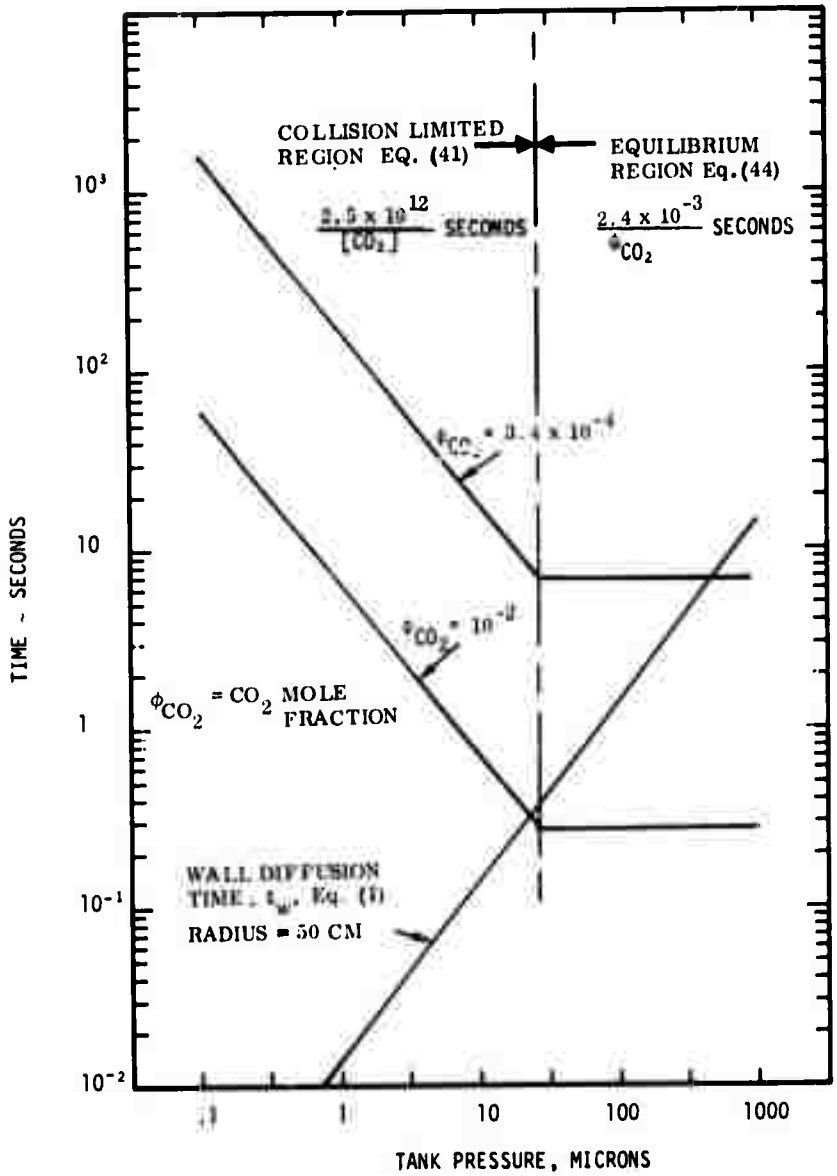

Figure 15. The time t_w for vibrationally excited nitrogen to diffuse to the wall as a function of the pressure. The time for N_2 vibrational energy to transfer to CO_2, for 3.4×10^{-4} and 10^{-2} CO_2 molefractions. When the wall is catalytic, the shorter time is appropriate for the experiment. Above 30 microns pressure the CO_2 radiating state is in equilibrium with the ground state, while at the lower pressures the population is depressed by radiation cooling.

where Equation (40) is used for ($[N_2^*]/[N_2]$). Sometimes the N_2 vibrational temperature, T_v, is used. This is defined

$$\exp(-3300°K/T_v) = [N_2^*] / [N_2] . \tag{46}$$

In the collision-limited region ($p < 30$ microns), the 4.3μ emission becomes

$$I_{4.3\mu} = (4\times10^{-13}) [CO_2] [N_2^*] \text{ photons/cm}^3 \text{ - sec} \tag{47}$$

$$= 4\times10^{-13} [N_2] [CO_2] \exp(-3300°K/T_v) \text{ photons/cm}^3\text{-sec}$$

Figure 16 gives the emission per cm^3 from the air. To convert from photon/sec to watts/steradian, multiply by:

$$\frac{1.6\times10^{-19}\times1.24}{4\pi\times4.3} = 4\times10^{-21}$$

We will now consider radiation in the 10 and 15 micron region. The CO_2(001) state can radiate to the ground state with 4.3 micron emission or to the (100) or (02°0) states with 10 micron emission. The radiation intensity is determined by the ratio of lifetimes,

$$\tau_{10\mu} = 5 \text{ sec and } \tau_{4.3\mu} = 3\times10^{-3} \text{ seconds.}$$

The intensity becomes

$$I_{10\mu} \begin{cases} = (3\times10^{-3}/5)I_{4.3} = 6\times10^{-4}\ I_{4.3} \text{ in photons/sec} \\ = (3\times10^{-3}/5)(4.3/10)I_{4.3} = (2.5\times10^{-4})I_{4.3} \text{ in watts/st} \end{cases} \tag{48}$$

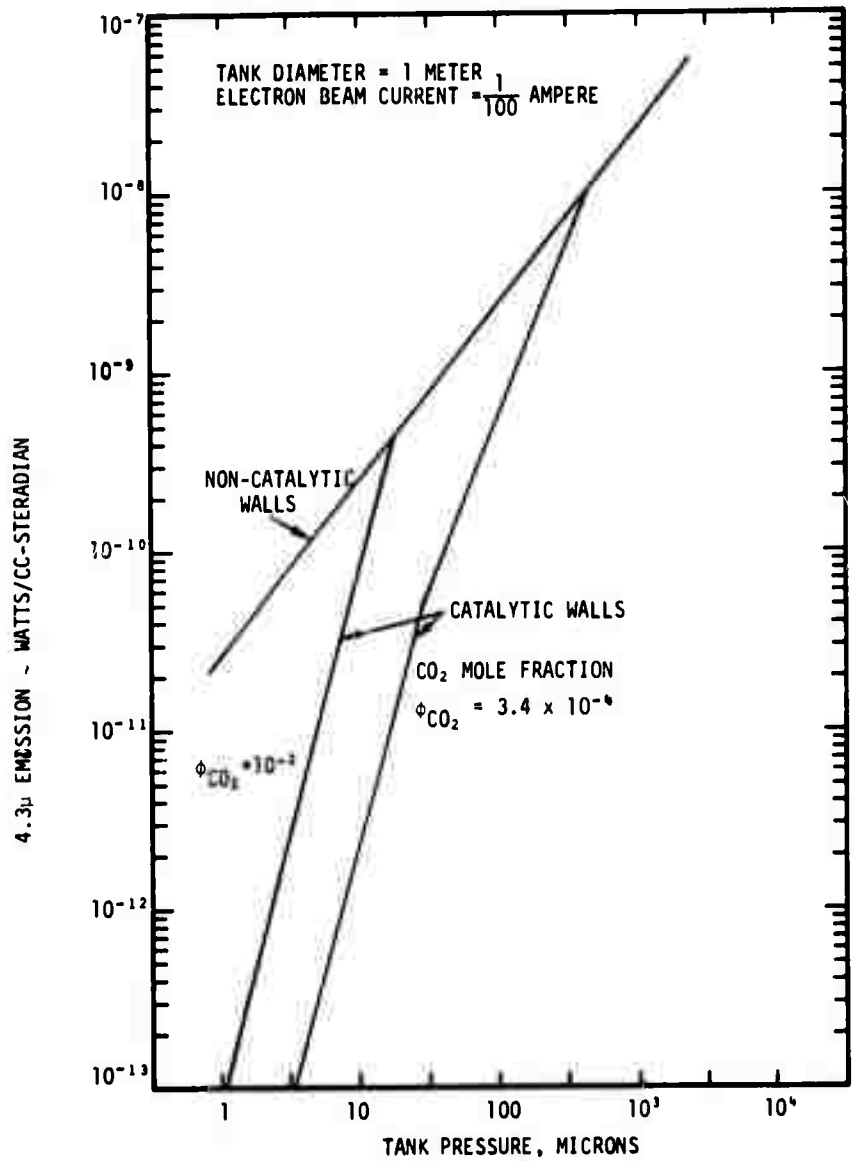

Figure 16. The CO_2 4.3 micron emission as a function of air pressure for a 1 meter diameter tank and an electron beam current of 10 milliamperes. The two cases presented are for a catalytic and non-catalytic wall to N_2 vibrational energy. For the non-catalytic wall, the excited nitrogen population builds up until transfer to CO_2. With the catalytic wall the transfer to CO_2 must occur before N_2 collisions with the wall. At low pressure the wall losses dominate, depressing the radiation.

For each 10 micron photon, there immediately follow two 15 micron photons due to the transitions from $(02^{o}0)$ to (000). The 15 micro intensity is

$$I_{15\mu} \begin{cases} = 1.2\times10^{-3}\ I_{4.3} \text{ in units of photons/sec} \\ = 3.3\times10^{-4}\ I_{4.3} \text{ in units of watts/st} \end{cases} \tag{49}$$

$I_{10\mu}$ and $I_{15\mu}$ can be determined by combining Equation (48) and (49) with the 4.3 micron intensity obtained from Figure 16. Direct electron excitation yields 15μ radiation in addition to $I_{15\mu}$ given by Equation (49). With the addition of water vapor in the gas there is additional infrared emission. The water vapor 6 micron radiation can be determined from the reactions with O_2 and N_2. The vibration exchange reactions are

$$N_2^* + H_2O(000) \rightarrow N_2 + H_2O(010) \qquad k = 10^{-17}\ cm^3/sec \tag{50}$$

$$O_2^* = H_2O(000) \rightarrow O_2 + H_2O(010) \qquad k = 3\times10^{-13}\ cm^3 sec \tag{51}$$

The main loss of oxygen vibrational energy would be through Reaction (51) which has the same reaction rate constant as the transfer between N_2 and CO_2. Thus, the $H_2O(6\mu)$ to $CO_2(4\mu)$ intensity ratio should be proportional to the species mole fraction ratio.

Other sources of infrared radiation could be NO, O_3, and NO_2 through Reactions (16) through (21). The most intense infrared emission occurs when NO is formed by Reaction (18), where the $N(^2D)$ is produced via Reaction (7). Reaction (16) proceeds too slowly at room temperature and can be neglected.

It is assumed that 2.7 photons are emitted in the 5.3 μ band per reaction $N(^2D) + O_2 \rightarrow NO^* + O$. Figure 17 presents the NO 5.3 μ emission in watts/cm^3 - sr as a function of the air pressure for a beam current of 10 milliamperes. The reaction rates for other infrared emitters are small requiring operation at 100 Torr pressure and at higher electron (100 ma) beam current. The ozone emission from Reaction (19) could be 3×10^{-11} watts cm^3 - sr, assuming a catalytic wall for atomic oxygen. The NO_2 emission obtained from Reaction (20) is expected to be similar to that obtained for ozone from Reaction (19). The infrared radiation from ozone can be studied by adding O_3 to the air. Figure 18 gives ozone radiation from a 1% ozone/99% air mixture. The radiation in the 9.6 micron band in watts/cm^3 - sr is shown as a function of tank pressure. Two methods for exciting ozone are presented: (1) vibration excitation by the electron beam, $e + O_3 \rightarrow e + O_3^*$, assuming the same excitation cross section as for N_2; and (2) vibration exchange between nitrogen and ozone, with the same exchange rate as between N_2 and CO_2. The break in the curve at about 20 microns pressure is due to the contribution from the back reaction. Figure 18 shows that measurable radiation levels can be produced and that O_3 vibrational excitation can be studied.

Neutral Bremsstrahlung

Free-free transitions produced in electron collisions between electrons and neutral molecules contribute some radiation in the infrared. The bremsstrahlung cross section for collision with neutrals is about two orders of magnitude less than for collisions with ions; however, the neutral number density is over 4 orders of magnitude larger than that for ions.

The free-free radiation from electron-neutral scattering is

$$I = (10^{-41}/\lambda^2 \sqrt{T})\, n_e [M]\, e^{-1.44/\lambda T} \text{ watts/cm}^3\text{-sr-}\mu$$

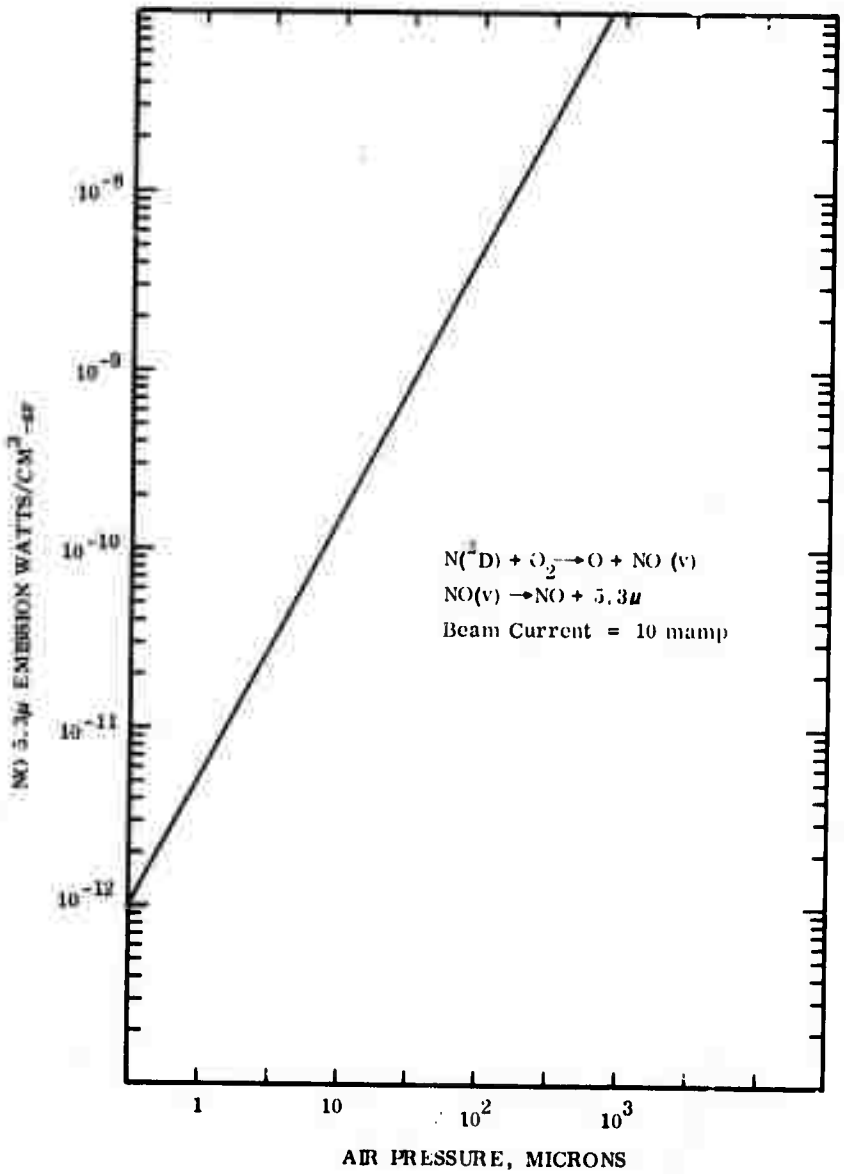

Figure 17. The NO 5.3 μ emission as a function of air pressure for a 1 meter diameter tank and 10 mamps electron beam current. The emission is due to the reaction $N(^2D) + O_2 \rightarrow NO(v) + O$ followed by 2.7 photons per reaction.

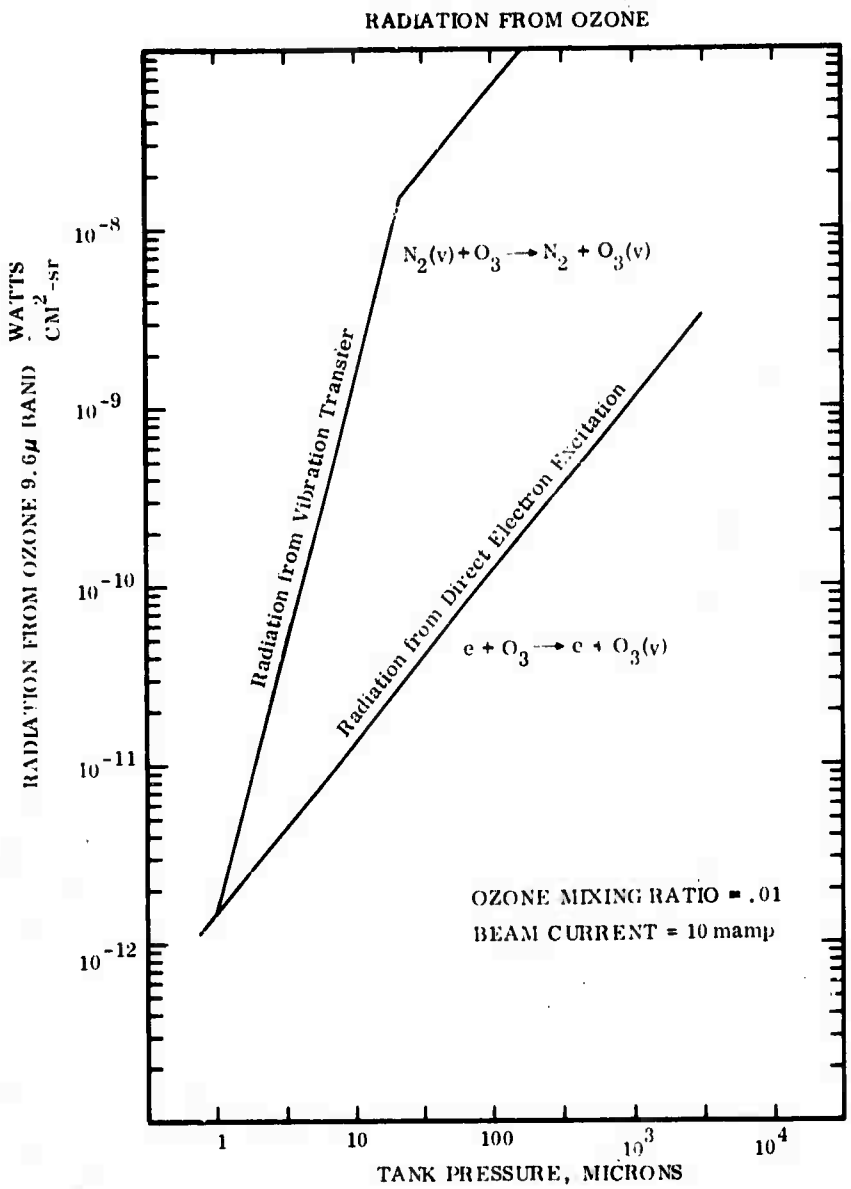

Figure 18. The O_3 9.6μ emission as a function of air pressure for a 1 meter tank and a 10 mamps electron beam current. The air contains 1% ozone. Three reactions were considered: vibration transfer from N_2 to O_3, direct O_3 vibration excitation by electrons, and the three-body recombination $O + O_2 + M \rightarrow O_3(v) + M$. The emission following the latter is below 10^{-13} watts/cm^2 sr.

where λ is the wavelength in cm; T the temperature in °K; n_e and [M] are the electron and neutral number density per cm^3. For $n_e = 10^{10}/cm^3$, [M] = $3 \times 10^{15}/cm^3$, $\lambda = 10^{-3}$ cm and T = 300 °K, then

$$I = (10^{-41})(10^6)(\frac{1}{17})(10^{10})(3.2\times10^{15})e^{-4.8}$$

$$= 1.5\times10^{-13} \text{ watts/cm}^3\text{-sr-}\mu = 1 \times 10^8 \text{ photons/cm}^3\text{-sec-}\mu$$

Free-free emission for this electron concentration is comparable with the level of detectability in this experiment.

The experimental arrangement shown in Figure 11 has a 1 meter source length and optical aperture of 15 cm. If the gas radiates J photons/cc-sec, then the radiation illuminating the detector S_D is

$$S_D = J\, \ell\, A_D / 4\pi f^2 \tag{52}$$

where ℓ is the thickness of radiating gas along the line of sight, A_D is the area of the detector and f is the f-number of the optics. For f = 2, $A_D = 0.1$ cm^2 and $\ell = 100$ cm, then $S_D = 0.2J$. Using detectors with $D^* = 10^{12}$ cm/w $\sqrt{\text{sec}}$ and a band pass of 1 Hz, the noise-equivalent-power becomes NEP = 3×10^{-13} watts $\approx$ 1.5×10^7 photons/sec. The minimum intensity J_m becomes

$$J_m = 5\, S_D = 5(S_D/\text{Noise})\ \text{Noise} = 15(\text{NEP}) = 2.3\times10^8 \text{ photons/cm}^3\text{-sec}$$

$$J_m = 6 \times 10^{-11} \text{ watts/cm}^3\text{-sr at } 10\mu$$

Here we have used a signal-to-noise ratio of 3. Thus, the NO, O_3, NO_2 and CO_2 intensities should be readily observable with the infrared system, since for these radiators $J > 10^{10}$ photons/cm^3 - sec.

Metastable States and Kinetics

The chemistry involving metastable species has been shown to be significant, e.g., the production of NO by the reaction $N(^2D) + O_2 \rightarrow NO + O$. We will estimate the concentrations of metastable species required for observation. Table II lists the metastable states in oxygen and nitrogen.[4] The second column gives the radiative lifetime. Most of these states have a faster collisional deactivation time. Columns 3, 4 and 5 treat collisional effects. Column 3 gives the collision partner with the fastest deactivation rate for the species concentrations in the tank. Columns 4 and 5 present the rate constants[4] and the deactivation time for 10 microns pressure. When the radiative lifetimes or collisional deactivation times are longer than the diffusion time to the wall (see Figure 3) then diffusion losses dominate. The last column are the metastable concentrations required for observation. This is based on a one meter optical path, 10^{-2} steradian optical system and 10^5 photoelectrons per second counting rate. The detectable concentration could be reduced significantly (by over an order of magnitude) using background suppression techniques and larger collection optics. Many of these metastable species should be observable in this experiment. The electron beam produces them in the dissociative recombination reactions and by secondary electron excitation.

While the discussion, so far, has considered the use of normal air ($0.2\text{-}O_2/0.8\text{-}N_2$), the system would be considerably more flexible. Mixtures such as $0.1\text{-}O/0.1\text{-}O_2/0.8\text{-}N_2$ could be used and these would be a better simulation of the atmosphere with 110 to 140 kilometers altitude range. The O atoms can be made in a discharge, in an iridium furnace, or by the reaction $N + NO \rightarrow N_2 + O$.

Table II. Comparison of Deactivation and Radiative Lifetimes[4]

Pressure = 10^{-2} Torr

	Radiative Lifetime, τ_r	Deactivation Processes			Metastable Concentration per cc (= $10^5\ \tau_r$)
		Collision with	Rate Constant	Deactivation Time Seconds	
$O_2(a^1\Delta_g)$	45 min	N	3×10^{-13} cc/sec	10^2	3×10^8
		O_2	10^{-18}	10^4	
$O_2(b^1\Sigma_g^+)$	12 sec	N_2	2×10^{-15}	1.5	10^6
$N_2(A^3\Sigma_u^+)$	2 sec	O_2	10^{-13}	0.15	2×10^5
		O	3×10^{-11}	1	
$N(^2D)$	26 hours	O_2	10^{-12}	0.015	10^{10}
$N(^2P)$	12 sec				10^6
$O(^1S)$	3/4 sec	O_2	2×10^{-13}	0.1	10^5
$O(^1D)$	110 sec	O_2	5×10^{-11}	.015	10^7
		N_2	8×10^{-11}	.003	
$O^+(^2P)$	5 sec				5×10^5
$O^+(^2D)$	3.5 hours	N_2	3×10^{-10}	.001	10^9
$N^+(^1S)$	0.9 sec				10^5
$N^+(^1D)$	4.13 min				2×10^7

The metastable $N(^2D)$ atoms can be produced readily by the addition of 1% (or less) NO. Charge exchange with N_2 quickly produces NO^+. $N(^2D)$ is then produced in the reaction $NO^+ + e \rightarrow N(^2D) + O(^3P)$. The importance of $N(^2D)$ chemistry in the enhancement of NO vibration excitation can be studied by changing the initial NO concentration.

In summary, there appears to be considerable flexibility in the choice of gases. The initial atom level could be varied and the effects of metastable states of N, O and O_2 could also be explored.

SUMMARY

This study investigated a laboratory experiment to simulate chemical and radiative auroral phenomena. Electron-beam illumination simulates auroral excitation by electrons. Other forms of auroral excitation such as electric currents and winds associated with electric fields are not considered. The main limitation of this experiment is depletion of some species by interactions with the wall. Long term chemical effects might not be observed because of the depletion of the active and metastable species by collisions with the walls. At the laboratory pressures, reactions with metastables are at a higher reaction rate than would occur at auroral altitudes where radiative processes depress the metastable population.

An important output of this experiment would be the measurement of infrared emission from air irradiated by electrons. The population of metastable states would be determined from their characteristic line emissions. The experiment would provide an important check for computer programs designed to model the gas chemistry and diffusion transport, and calculate the expected emissions. This experiment would check the integral chemistry; that is, identify the important species and their reaction paths, and the dominant radiators and spectral characteristics.

While most of the experiment would be done in N_2 - O_2 mixtures, a variety of important chemical reactions could be explored by starting with mixtures of O - O_2 - N_2, or with small amounts of other species, such as O_3, NO, H_2O and CO_2. Infrared emission can be measured from the following species: NO, O_3, CO_2, H_2O and NO_2.

While the main emphasis in this study has been placed on the infrared emission, additional information could be obtained. The N_2 first negative radiation gives the distribution of the energy deposition by the electron beam, and the N_2 vibrational and translational temperatures. Mass spectroscopy would determine the ionic and neutral species concentrations.

Preceding page blank

The analyses assumed that losses to the wall are determined by only diffusion, ignoring convection currents. Estimates of convection cooling indicate that it becomes important at beam currents in excess of 100 milliamperes and pressures above 100 microns. Thus, convection losses would be unimportant over the proposed operating range.

The analyses assumed that losses to the wall are determined by only diffusion, ignoring convection currents. Estimates of convection cooling indicate that it becomes important at beam currents in excess of 100 milliamperes and pressures above 100 microns. Thus, convection losses would be unimportant over the proposed operating range.

REFERENCES

1. Murcray, David G., Optical Properties of the Atmosphere, Six-Month Technical Report (Contract F19628-68-C-0233), University of Denver, January 1971

2. Hartman, Paul L., New Measurements of the Fluorescence Efficiency of Air Under Electron Bombardment, Pergamon Press, Planet. Space Sci., 16, 1315 (1968)

3. Harris, I & Priester, W., The Upper Atmosphere in the Range from 120 to 800 km. Reprinted in COSPAR International Reference Atmosphere, North-Holland Publ. Co., Amsterdam (1965)

4. Zipf, E. C., The Collisional Deactivation of Metastable Atoms and Molecules in the Upper Atmosphere, Canadian Journal of Chemistry, 47, 10 (1969)

5. Bortner, M. & Kummler, R., The Chemical Kinetics and the Composition of the Earth's Atmosphere, General Electric Scientific Rpt. #1, 24 July 1968

6. Cohn, A. & Caledonia, G., Spatial Distribution of Fluorescent Radiation Emission caused by an Electron Beam, J. of Applied Physics, 41, 3767 (1970)

7. DASA Reaction Rate Hand Book, July 1967

8. O'Neil, R. R., Pendleton, W. R., Jr., Hart, A. M., and Stair, A. T., Jr., "Measurement of Vibrational Temperature of Atmospheric Nitrogen by Means of Electron Beam Induced Luminescence," Radiating Atmosphere edited by B. McCormac, D. Reidel Publishing Co., Holland, 1971

9. Jobe, J. D., Sharpton, F. A., & St. John, R. M , Apparent Cross Sections of N_2 for Electron Excitation of the Second Positive System, J. of the Optical Society of America, 57, 106 (1967)

10. Clup, G. & Stair, A. T., Jr., Effective Rotational Temperatures of N_2^+ (3914 A) Excited by Monoenergetic Electrons in A Crossed Beam, Extrait du Journal de Chimie Physique, #1, p. 57 (1967)

11. Norton, Richard B., Theory of Nitric Oxide in the Earth's Atmosphere, J. of Geophysical Research, Space Physics, 75, No. 19, July 1, 1970